USGS
science for a changing world

Mapping Ground Water in Three Dimensions—An Analysis of Airborne Geophysical Surveys of the Upper San Pedro River Basin, Cochise County, Southeastern Arizona

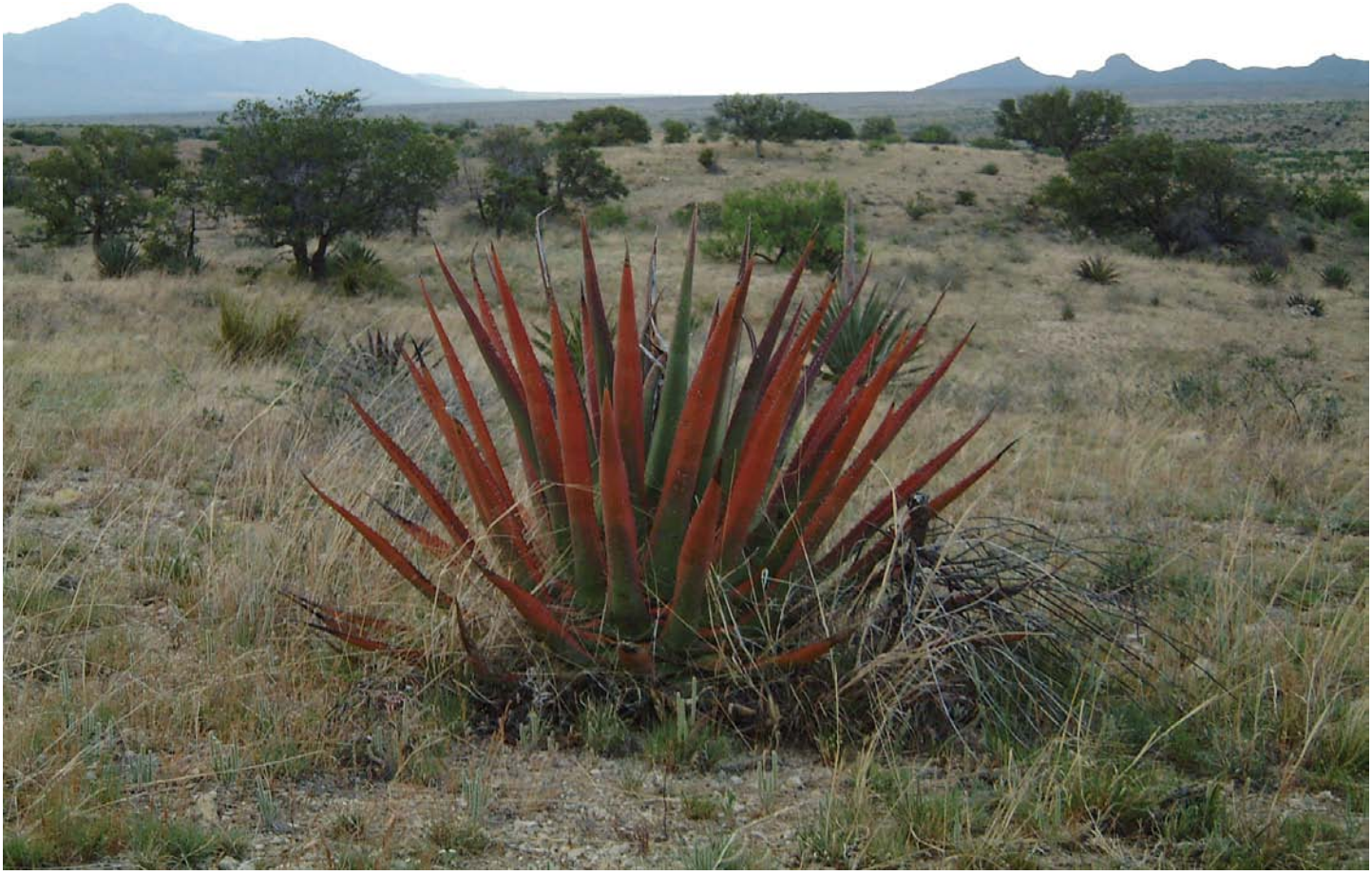

Professional Paper 1674

U.S. Department of the Interior
U.S. Geological Survey

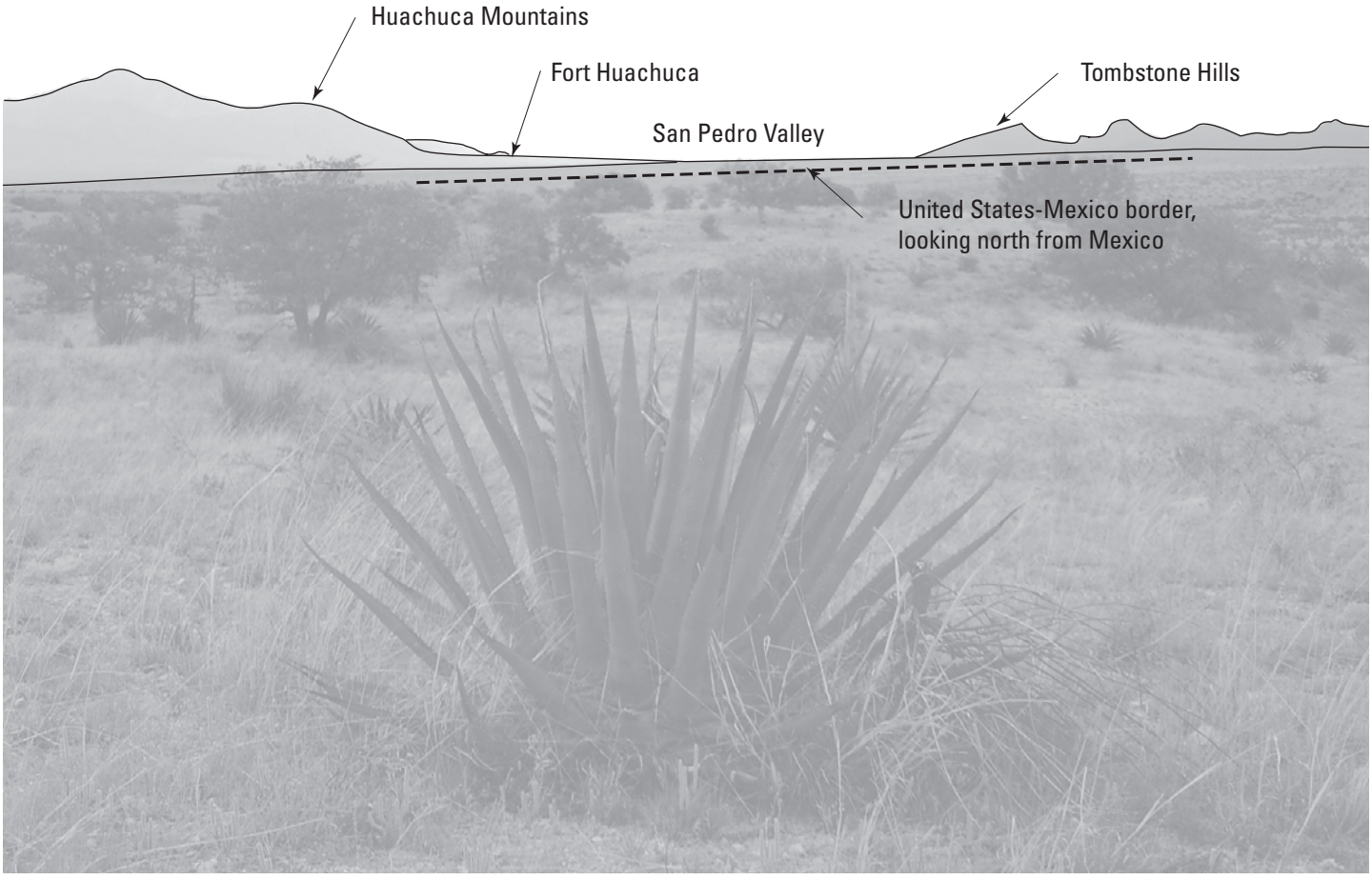

Cover. View of the upper San Pedro Valley, looking north from Mexico.

Mapping Ground Water in Three Dimensions—An Analysis of Airborne Geophysical Surveys of the Upper San Pedro River Basin, Cochise County, Southeastern Arizona

By Jeff Wynn

Supersedes Open-File Report 00–517

Professional Paper 1674

U.S. Department of the Interior
U.S. Geological Survey

U.S. Department of the Interior
DIRK KEMPTHORNE, Secretary

U.S. Geological Survey
Mark D. Myers, Director

U.S. Geological Survey, Reston, Virginia: 2006

For product and ordering information:
World Wide Web: http://www.usgs.gov/pubprod
Telephone: 1–888–ASK–USGS

For more information on the USGS—the Federal source for science about the Earth, its natural and living resources, natural hazards, and the environment:
World Wide Web: http://www.usgs.gov
Telephone: 1–888–ASK–USGS

Suggested citation:
Wynn, Jeff, 2006, Mapping ground water in three dimensions—An analysis of airborne geophysical surveys of the upper San Pedro River basin, Cochise County, southeastern Arizona: U.S. Geological Survey Professional Paper 1674, one CD-ROM. (Also available online.)

Library of Congress Cataloging-in-Publication Data

Wynn, Jeffrey C.
Mapping ground water in three dimensions : an analysis of airborne geophysical surveys of the Upper San Pedro River Basin, Cochise County, Southeastern Arizona / by Jeff Wynn.
p. cm. –(Professional paper ; 1674)
"Supersedes Open–File Report 00–517."
Includes bibliographical references.
1. Groundwater—San Pedro River Watershed (Mexico and Ariz.)—Remote sensing. 2. Groundwater—Arizona—Remote sensing. 3. Aerial photography in hydrogeology. I. Title.
GB1025.A6W96 2006
551.4909791'53—dc22

2006041319

ISBN 1-411-30901-4

Contents

Abstract 1
Introduction and Background....1
Previous Hydrological, Geological, and Geophysical Studies 4
Data Acquisition for the Airborne Geophysical Surveys 5
Quality Control Analysis....8
Magnetic Data and Depth-to-Basement 10
The Airborne EM Data and Water in the San Pedro River Basin 14
Conductivity Depth Transforms 23
Conductivity vs. Depth Conversion Systems—The Inversion "Tuning" Issue 26
Summary of Interpretations 28
Interpretations Related to the Hydrology of the Upper San Pedro Drainage Derived from the Airborne EM and Magnetic Data....28
Observations about the Geology of the Upper San Pedro Drainage Derived from the EM and Magnetic Data 30
Observations about the Geophysical Methods, Including the CDT Conversion Process....31
Acknowledgments....31
References Cited....31

Plates

1. Depth to water table superimposed on shallow (1999 EM channel 10) conductivity data plotted on a map of the Fort Huachuca area, Arizona (an enlarged version of text figure 17)
2. Conductivity vs. depth fence diagram superimposed on a topographic map of the Fort Huachuca area, Arizona (an enlarged version of text figure 22)

Figures

1. Index map of Arizona showing the locations of the 1997 San Pedro and 1999 Tombstone airborne geophysical surveys....2
2. Map showing boundaries of the four discrete airborne geophysical surveys (one during 1997 and three during 1999) superimposed on a topographic map of the Fort Huachuca area, Arizona....3
3. Map showing survey lines and survey parameters for the three 1999 Tombstone airborne geophysical survey segments adjacent to the survey lines from 1997 6
4. Combined 1997 and 1999 aircraft survey lines superimposed on a topographic map of the Fort Huachuca area, Arizona 7
5. Graph showing altimeter calibration for the 1999 airborne geophysical survey 9
6. Measured radar altimeter variations superimposed on a shaded-relief topographic map of the Fort Huachuca area, Arizona, with contour lines of the 1999 EM channel 10 (*z*-axis) conductivity 10
7. Radar altimeter variations superimposed on the 1999 EM channel 10 (*z*-axis) conductivity, over a shaded-relief topographic map of the Fort Huachuca area, Arizona ...11

8. Radar altimeter variations superimposed on a contoured shaded-relief topographic map of the Fort Huachuca area, Arizona 12
9. Aeromagnetic data map showing merged magnetic data from the 1997 San Pedro and 1999 Tombstone airborne geophysical surveys for the Fort Huachuca area, Arizona....13
10. Euler deconvolution solutions superimposed on a topographic map of the Fort Huachuca area, Arizona 14
11. Map of the Fort Huachuca area, Arizona, showing magnetic depth-to-source data (crystalline basement in most cases) from Euler deconvolution of magnetic data (Hanning filtered for clarity) for a structural index of 0 15
12. Map of the Fort Huachuca area, Arizona, showing depth-to-basement data derived from modeling gravity data 16
13. Thematic Mapper image of the Sierra Vista subbasin of the upper San Pedro River drainage....17
14. Map of the Fort Huachuca area, Arizona, showing combined results from the 1997 and 1999 airborne EM surveys, *z*-axis component, for channel 10 18
15. Map of the Fort Huachuca area, Arizona, showing combined results from the 1997 and 1999 airborne EM surveys, *z*-axis component, for channel 14 19
16. Map of the Fort Huachuca area, Arizona, showing combined results from the 1997 and 1999 airborne EM surveys, *z*-axis component, for channel 18 20
17. Depth to water table superimposed on shallow (1999 EM channel 10) conductivity data plotted on a map of the Fort Huachuca area, Arizona....22
18. An example CDT profile from survey line 122, with an interpretation superimposed....23
19. Graph showing comparison of resistivities derived from the airborne EM survey CDT with resistivities derived from a well log for test well 5 24
20. Graph showing CDT vertical profiles plotted against water-table information and well-resistivity data (log base 10 of resistivity) for nine test wells....25
21. Comparison of two CDT profiles (1997 line 101 and 1999 line 214) that approximately coincide 26
22. Conductivity vs. depth fence diagram superimposed on a topographic map of the Fort Huachuca area, Arizona 27
23. A comparison of a true inversion of the 60-channel EM data (using an EM Flow CDI) with a Geoterrex-Dighem CDT profile for the same survey line 29

Tables

1. Electromagnetic time-domain gates in the 1999 airborne electromagnetic survey....8
2. Channel equivalencies between the 1997 and 1999 airborne electromagnetic surveys....8

Conversion Factors

Multiply	By	To obtain
	Length	
centimeter (cm)	0.3937	inch (in.)
meter (m)	3.281	foot (ft)
kilometer (km)	0.6214	mile (mi)
	Volume	
cubic meter (m^3)	0.0008107	acre-foot (acre-ft)

Specific conductance (conductivity) of ground water is given in microsiemens per centimeter (µS/cm).

Electromagnetic (EM) conductivity is given in parts per million of the secondary (momentary) field strength divided by the primary field strength.

Resistivity is given in ohm-meters. Resistivity measures the extent to which a material offers resistance to passage of an electric current. The resistivity of a conductor in ohm-meters is defined to be its resistance (in ohms) multiplied by its cross-sectional area (in square meters) divided by its length (in meters).

Amplitude of transmitter signal current is given in amperes.

Magnetic dipole moments per unit volume are given in amperes per meter.

Frequency is given in hertz (equal to one cycle per second).

Electric potential (airborne electromagnetic signal) is measured in picovolts per square meter. Pico denotes 10^{-12} (one-trillionth).

Mapping Ground Water in Three Dimensions—An Analysis of Airborne Geophysical Surveys of the Upper San Pedro River Basin, Cochise County, Southeastern Arizona

By Jeff Wynn

Abstract

This report summarizes the results of two airborne geophysical surveys conducted in the upper San Pedro Valley of southeastern Arizona in 1997 and 1999. The combined surveys cover about 1,000 square kilometers and extend from the Huachuca Mountains on the west to the Mule Mountains and Tombstone Hills on the east and from north of the Babocomari River to near the Mexican border on the south. The surveys included the acquisition of high-resolution magnetic data, which were used to map depth to the crystalline basement rocks underlying the sediments filling the basin. The magnetic inversion results show a complex basement morphology, with sediment thickness in the center of the valley ranging from ~237 meters beneath the city of Sierra Vista to ~1,500 meters beneath Huachuca City and the Palominas area near the Mexican border. The surveys also included acquisition of 60-channel time-domain electromagnetic (EM) data. Extensive quality analyses of these data, including inversion to conductivity vs. depth (conductivity-depth-transform or CDT) profiles and comparisons with electrical well logs, show that the electrical conductor mapped represents the subsurface water-bearing sediments throughout most of the basin.

In a few places (notably the mouth of Huachuca Canyon), the reported water table lies above where the electrical conductor places it. These exceptions appear to be due to a combination of outdated water-table information, significant horizontal displacement between the wells and the CDT profiles, and a subtle calibration issue with the CDT algorithm apparent only in areas of highly resistive (very dry) overburden. These occasional disparities appear in less than 5 percent of the surveyed area. Observations show, however, that wells drilled in the thick unsaturated zone along the Huachuca Mountain front eventually intersect water, at which point the water rapidly rises high into the unsaturated zone within the wellbore. This rising of water in a wellbore implies some sort of confinement below the thick unsaturated zone, a confinement that is not identified in the available literature. Occasional disparities notwithstanding, maps of the electrical conductor derived from the airborne EM system provide a synoptic view of the presence of water underlying the upper San Pedro Valley, including its three-dimensional distribution. The EM data even show faults previously only inferred from geologic mapping.

The magnetic and electromagnetic data together appear to show the thickness of the sediments, the water in the saturated sediments down to a maximum of about 400 meters depth, and even places where the main ground-water body is not in direct contact with the San Pedro River. However, the geophysical data cannot reveal anything directly about hydraulic conductivity or ground-water flow. Estimating these characteristics requires new hydraulic modeling based in part on this report.

One concern to reviewers of this report is the effect that clays may have on the electrical conductor mapped with the airborne geophysical system. Although the water in the basin is unusually conductive, averaging 338 microsiemens per centimeter, reasoning cited below suggests that the contribution of clays to the overall conductivity would be relatively small. Basic principles of sedimentary geology suggest that silts and clays should dominate the center of the basin, while sands and gravels would tend to dominate the margins. Although clay content may increase the amplitude of the observed electrical conductors somewhat, it will not affect the depths to the conductor derived from depth inversions. Further, fine-grained sediments generally have higher porosity and tend to lie toward a basin center, a fact in general agreement with the observed geophysical data.

Introduction and Background

The upper San Pedro Valley in southeastern Arizona is an area of concern for ground-water resources, in part due to its natural aridity and in part due to multiple competing land uses. These land uses include commercial development, ranching, military base activities, and the San Pedro National Riparian Conservation Area (SPNRCA). Congress established the

SPNRCA in 1988 under the Arizona-Idaho Conservation Act (Public Law 100–696); among other things, this act set Federal reserve water rights for minimum flows in the river. In early 1997, the U.S. Army requested that an airborne electromagnetic survey (Geoterrex-Dighem, 1997) be flown over the Fort Huachuca Military Reservation and immediate surrounding areas (Defense Mapping Agency, 1994; Wynn and Gettings, 1997; Bultman, Gettings, and Wynn, 1999). This survey was designed to provide detailed three-dimensional information on the regional aquifer of the upper San Pedro River drainage.

Due to this initial success, in early 1999 a followup airborne geophysical survey (Geoterrex-Dighem, 1999) was flown over three adjacent land tracts (fig. 1). In addition, an experimental line was flown east-west across the San Pedro Valley near the Mexican border to help document structure and stratigraphy of the sediments and to locate the aquifer in the vicinity of the international boundary. Survey outlines are shown in figure 2; note that, in this and subsequent figures, the coordinate system used is Universal Transverse Mercator (UTM) zone 12. These surveys were designed and carried out under U.S. Geological Survey (USGS) supervision (see "Acknowledgments").

These surveys were planned to gather resistivity data from the upper 150–400 meters of the subbasin to help map the regional aquifer and the geologic structures that might control ground-water flow. (Note that the four separate survey segments were merged for this report.) In addition, the surveys acquired magnetic data, which were used to develop a map of the magnetic field strength. This map helps define the location of faults and fractures in the crystalline rocks forming the basement beneath the sediments (and, in some cases, volcanic rocks within the basin fill). The magnetic data can also be used to estimate depth-to-source of the crystalline basement rocks and, thus, to provide another set of estimates (in addition to the existing, relatively coarsely spaced gravity data) of the basin's sediment fill. The thickness of sediments bears significantly on the hydrology of the basin, as shallow crystalline basement may interfere with water flow.

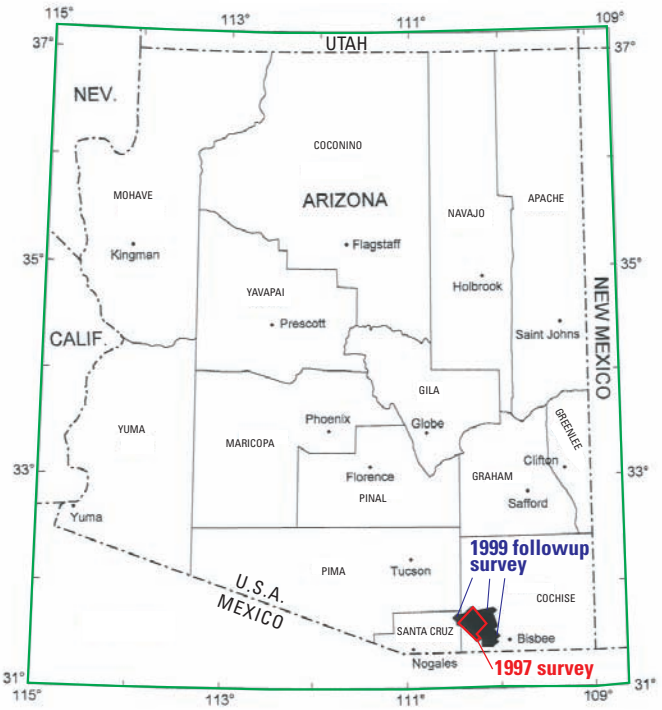

Base derived from U.S. Geological Survey DLG. UTM zone 12.

Figure 1. Index map of Arizona showing the locations of the 1997 San Pedro and 1999 Tombstone airborne geophysical surveys.

Brown and others (1966) identified two different basin fill units that constitute the regional aquifer: the relatively more porous upper basin fill and the more consolidated, less porous underlying lower basin fill. Recharge to the regional aquifer in the Sierra Vista subwatershed of the upper San Pedro ground-water basin (defined as the part of the San Pedro drainage bounded by the Mexican border on the south and the northern extents of the Babocomari River and Walnut Gulch drainages on the north and by the Huachuca Mountains on the west and the Mule Mountains on the east) is estimated to be about 15.4 million to 18.5 million cubic meters a year, primarily from the Huachuca Mountains and to a lesser extent from the Mule Mountains and the Tombstone Hills (fig. 2; see Freethey, 1982; Pool and Coes, 1999). In addition, Mexico contributes up to 4.3 million cubic meters per year of ground-water flow (Freethey, 1982).

Ground-water withdrawal from the Sierra Vista subwatershed was probably less than 13.6 million cubic meters per year in 1991 (Corell and others, 1996). It peaked at around 18.5 million cubic meters per year in the early 1980s but has declined since then due in part to conservation measures, but principally due to the retirement of irrigation pumping. In addition, evapotranspiration along the San Pedro River by phreatophyte vegetation (for example, cottonwoods, mesquite, and willow trees that use ground water) is estimated to be about 7.6 million cubic meters a year (Freethey, 1982; Pool and Coes, 1999). Also, ground-water discharge to the San Pedro River is about 7.3 million cubic meters annually (Freethey, 1982). Total input to the ground-water system is about 22 million cubic meters per year. A total outflow from the system of about 27.2 million cubic meters per year results in depletion of ground-water storage. More importantly, ground-water withdrawals intercept the flow of ground water to the river and riparian area. Significant interception of the flow will affect river flow and will lead to an inevitable reduction in riparian vegetation. The ground-water deficit varies from year to year, depending on climate, withdrawals, recent conservation measures, and consumption by large mines and communal farms (ejidos) in Mexico.

Extensive fine-grained silt and clay layers have been identified in the regional aquifer (Pool and Coes, 1999). These fine-grained sediments tend to dominate the center of the San Pedro Valley, consistent with being more distal from their weathering origins in the Huachuca and Mule Mountains, and they influence the ground-water flow and interactions between the regional aquifer and the San Pedro River. The fine-grained

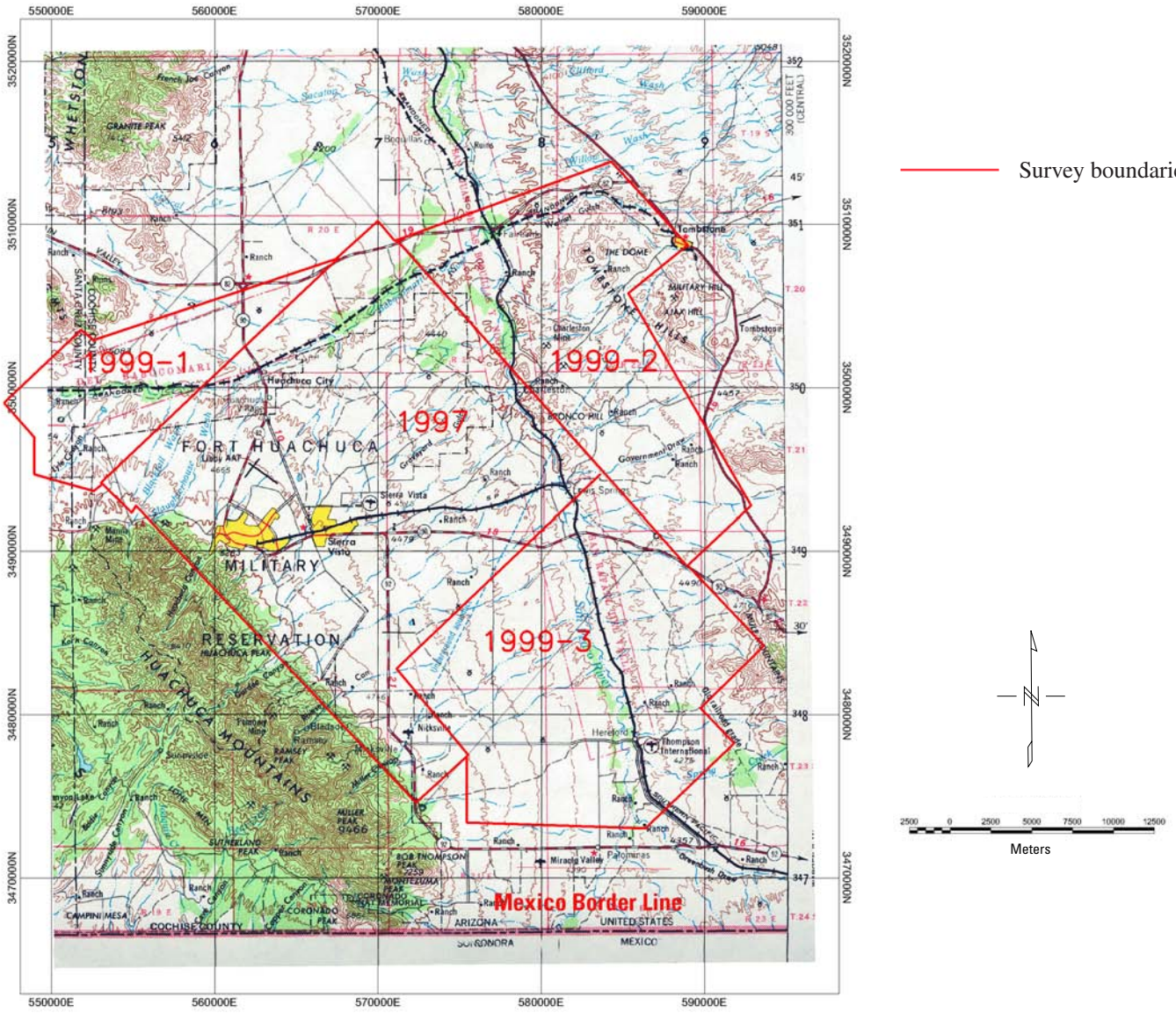

Base from U.S. Geological Survey 1:250,000-scale topographic map series. UTM zone 12.

Figure 2. Map showing boundaries of the four discrete airborne geophysical surveys (one during 1997 and three during 1999) superimposed on a topographic map of the Fort Huachuca area, Arizona. Red lines indicate survey boundaries. An experimental profile (10 kilometers long) flown east-west across the San Pedro Valley near the U.S.-Mexico border is denoted by the words in red, "Mexico Border Line"; see also figures 3 and 22 and plate 2.

sediments are overlain and underlain by saturated sands and gravels (W. Steinkampf, U.S. Geological Survey, Tucson, Ariz., written commun., 2000). Water-level data from wells and several springs to the west of the San Pedro River indicate that the water table becomes increasingly shallow toward the San Pedro River and that ground water discharges as spring flow in places west of the river (Pool and Coes, 1999). Conductivity maps and conductivity-depth-transform (CDT) profiles discussed below suggest that parts of the San Pedro River in the vicinity of the Tombstone volcanic rocks (as mapped by Moore, 1993) are not in direct hydraulic contact (defined as saturated flow between aquifer and river) with the Sierra Vista subwatershed of the upper San Pedro River basin ground-water system.

This report describes the airborne geophysical surveys, summarizes the operating parameters for the survey system, and outlines the steps taken to assess quality of the merged datasets. It includes a section describing calculations of depth-to-source from the magnetic data (primarily addressing the depth to the crystalline basement underlying the San Pedro basin sediments). The report then shows several ways in which the combined 1997/1999 airborne electromagnetic (EM) data can be viewed to understand the three-dimensional aspects of the regional aquifer in the Sierra Vista subwatershed.

Water-table depths (http://www.azwater.gov/dwr/content/Find_by_Program/Wells/default.htm; see also the USGS National Water Information System Web site (NWISWeb) at http://nwis.waterdata.usgs.gov/nwis) are then compared with the shallow electrical conductor derived from the airborne electromagnetic survey. The water-table information dates from the 1970s through the 1990s; only the most recent value for a given well was used, but some depths have not been measured for several decades. Finally, a section of the report discusses the issue of inversion of the electromagnetic data into conductivity-depth-transform profiles (CDTs, or conductivity vs. depth), what CDT profiles tell us about the aquifer, and how reliable these inversions might be. A second method of doing inversions from the airborne EM data was tested and compared with the CDT results. Estimation of depth to water from these inversions was generally quite good, especially when compared to depths from electrical well logs. With a few exceptions discussed below, the CDTs for the entire survey area show maximum amplitude of the conductor at the water.

In the following discussion, the electrical properties of sediments are described in terms of conductivities, specifically in units of microsiemens per centimeter (μS/cm). This metric makes viewing the EM maps easier for the reader: red/purple hues in images shown later represent higher conductivity and show where the water is concentrated, as verified by comparison to electrical well logs. In general, higher clay content gives an increased conductor amplitude, represented by the darker purple colors. The blue in the images represents lower conductivity, generally unsaturated zones and crystalline rock. Most ground geophysical measurements are reported as resistivity values (in ohm-meters). The relation between the two is straightforward: conductivity = 1/resistivity (for example, 200 μS/cm = 50 ohm-meters).

Previous Hydrological, Geological, and Geophysical Studies

A number of hydrologic studies of the upper San Pedro River basin have been produced over the years; one of the earliest was by Brown and others (1966). Brown and others described an upper basin fill, a lower basin fill, and an underlying, older Pantano Formation lying on crystalline basement. The upper basin fill and lower basin fill are lithologically similar; the main difference between them is relative porosity. Freethey (1982) provided the original ground-water model, on which all subsequent models have been based. The most recent studies include detailed hydrologic models, such as one developed by the Arizona Department of Water Resources (Corell and others, 1996). Previous conceptual and numerical models assumed a fairly simple basin structure; however, in a subsequent section of this report, the reader will encounter a more complex basement configuration derived from aeromagnetic data acquired from the 1997 and 1999 airborne geophysical surveys.

Pool and Coes (1999) conducted the most recent hydrologic study of the San Pedro regional aquifer. They identified extensive fine-grained units in the regional aquifer and provided detailed hydrogeologic sections of the sediments in the Sierra Vista subwatershed of the upper San Pedro River basin that were based on well data and vertical electrical soundings. Pool and Coes (1999) defined the primary regional aquifer as including "upper and lower basin fill, described by Brown and others (1966), that accumulated in the structural depression between mountain ranges during the Miocene through early Pleistocene ages." Figure 8 of Pool and Coes (1999) is particularly helpful as an overview of the sedimentary package hosting the regional aquifer.

Drewes (1980) completed a regional geologic and tectonic map, supplemented in part by wilderness maps of the Coronado National Forest (Drewes, 1996; Sean Kneale and others, U.S. Forest Service, written commun., 1997). A 1:50,000-scale geologic map by Moore (1993) outlines a newly discovered volcanic complex and shows that parts of a large collapse caldera margin (part of what is now generally designated the Tombstone caldera) underlie the eastern margins of the Fort Huachuca Military Reservation near the San Pedro River, including land covered by the airborne geophysical surveys. Together, these reports forced a fundamental reconsideration of the subbasin structure. Reports by Halvorson (1984), Gettings and Houser (1995, 2000), and Gettings and Gettings (1996) provide an approximate map of the depth to bedrock beneath the Tertiary-Quaternary basin fill underlying the upper San Pedro River drainage (compared below with depth-to-source maps derived from the airborne magnetic data). These earlier studies revealed a depression in the bedrock as much as a kilometer deep beneath Huachuca City and shallow crystalline rock underlying parts of the city of Sierra Vista. This latter structural high appears to be an uplifted basement block; this interpretation is supported by a driller's log of well D(21-20)35abb, where crystalline basement was encountered 237 meters deep near Fry Boulevard in downtown Sierra Vista. Euler deconvolution of aeromagnetic data (detailed below) also supports and augments information on these structures in the underlying crystalline basement. A seismic-reflection study designed to map the water table and the aquifer (Environmental Engineering Consultants, 1996) gave inconclusive results.

No previous airborne electromagnetic surveys over the area are known to exist. Pool and Coes (1999) collected and analyzed ground-based electric soundings and profiles at selected sites in the area, and the area is included in earlier regional aeromagnetic surveys at 1.6-kilometer spacing between flightlines (Andreasen and others, 1965) and proprietary mining company data at 0.5-kilometer spacing. Geophysical logs of nine test wells on the Fort Huachuca Military Reservation are available (U.S. Army Corps of Engineers, 1972, 1974) and were used for evaluation of the 1997 airborne geophysical survey data covering the center of the study area (Wynn and Gettings, 1997; Bultman, Gettings, and Wynn, 1999). The Arizona Department of Water Resources pro-

vided a digital dataset of water-well locations and depths to water measured within the last few years for comparison to the electromagnetic data interpretation (also available in the USGS NWISWeb database). Gettings and Gettings (1996) collected and interpreted a detailed ground magnetic profile from the Dragoon Mountains southwest across the valley to the east gate of Fort Huachuca. Halvorson (1984) conducted the first gravity survey to map the depth to basement in the San Pedro Valley, followed by Gettings (1996). Gettings and Houser (2000) collected, compiled, and interpreted gravity anomaly, water-resources, exploration borehole geologic logs, and surface geologic data to model the depth and shape of the basin in the Sierra Vista to Huachuca City area. Significant amounts of proprietary geologic, geophysical, and geochemical data have been collected by mineral exploration companies for areas of bedrock outcrop, but these data were not available to the author.

Data Acquisition for the Airborne Geophysical Surveys

The 1999 airborne geophysical survey (Geoterrex-Dighem, 1999; referred to as the "Tombstone survey" to distinguish it from the Geoterrex-Dighem, 1997, "San Pedro survey") was conducted from February 22 to March 1, 1999, and acquired both electromagnetic and magnetic data. Three discrete areas were flown to supplement coverage from the 1997 San Pedro airborne geophysical survey of Fort Huachuca and surrounding areas (reported in Wynn and Gettings, 1997; Bultman, Gettings, and Wynn, 1999). Areas 1–3 are labeled 1999–1, 1999–2, and 1999–3, respectively, in figure 2 and extend from Lyle Canyon to the city of Tombstone in the north, to the Mule Mountains and Greenbush Draw on the east, and over to the Huachuca Mountains on the south about 8 kilometers from the Mexican border (Wynn and others, 2000; Wynn, 2002). In addition, a single experimental 10-kilometer-long profile was flown parallel to, but approximately 3 kilometers north of, the Mexican border to monitor ground water between the headwaters of the upper San Pedro drainage in Mexico and the regional aquifer in the Arizona part of the study area (see p. 26 and pl. 2).

The data were seamlessly merged with the 1997 survey, with the exception of the single experimental profile (analyzed in detail at the end of this report). A total of 1,366 kilometers of data were acquired, including 620 kilometers in Area 1, 283 kilometers in Area 2, and 454 kilometers in Area 3. Line-spacing in Areas 1 and 2 was ~400 meters; Area 3 was flown at 800-meter spacing to fit within survey contract specifications but also to maximize the areal coverage on the southern margin of the survey. Figure 3 shows the flightline spacing (400 meters and 800 meters), the flightline orientation for each segment, and the total kilometers covered in each section. Figure 4 shows the line-coverage superimposed on the local roads and topography for reference.

The survey used a CASA C–212 twin turbo-prop aircraft, with nominal survey flight speed of about 125 knots (65 meters per second), flown at a nominal terrain-clearance of 120 meters. A Rosemount 1241M barometric altimeter was used to control survey aircraft elevation; this unit has a sensitivity of about 0.3 meter in a 1-second recording interval. The radar altimeter was a TRT AHV–8 model having 2 percent accuracy over a 0- to 800-meter range; it also had a 1-second recording interval. A Panasonic Super (VHS) camera (model WV–CL302) was used to aid navigational recovery and help identify cultural interference. Electronic navigation was maintained to a horizontal precision of 10 meters by using a Sercel differential Global Positioning System (GPS) receiver (model NR103). This GPS system sampled locations once every second to a resolution of 0.00001 degree.

The magnetic data were acquired by using a Scintrex CS–2 single-cell cesium-vapor magnetometer, which was trailed in a towed sonde called a "bird" behind the aircraft and which sampled at 0.1-second intervals. This sampling interval gives a magnetic data density of about one sample per 6.5 meters. Nominal sensor height was 73 meters above ground. The contractor estimated that the noise envelope for this survey was about ±0.5 nanoteslas (nT). A base station magnetometer was also operated at the Fort Huachuca airport to provide data for the diurnal magnetic field correction. The contractor completed corrections to the magnetic field data for diurnal drift, for sensor lag (sensor distance behind GPS antenna), for leveling (tie-line intersections), and for subtraction of the International Geomagnetic Reference Field computed at an altitude of 1,430 meters above mean sea level. The contractor also supplied the magnetic field data as digital files of data along the flightlines on a grid having an interval of 50 meters.

The GEOTEM Airborne ElectroMagnetic (AEM) System is a proprietary EM exploration system available only from Geoterrex-Dighem. The system uses a transmitter coil of 232 square meters with six turns, flown at a nominal height above ground of 120 meters. The transmitter signal-current was an unusual time-domain signal (a 4,080-microsecond half-sine followed by a 12,486-microsecond flat off-time) having an amplitude of 500 amperes. The dipole moment was 6.96×10^5 amperes per meter. The multicoil (three-axis: *x*, *y*, and *z*) receiver system was towed behind the aircraft in a bird maintained about 70 meters above the ground surface and approximately 125 meters behind the transmitter coil center. For maximum penetration of the underlying sediments, the system was set to operate with a base frequency of 30 hertz (cycles per second); this provides a transmitter pulse width of 4,080 microseconds.

The *x*-axis (in-line) and *y*-axis (side-looking) receiver components were optimally coupled for detecting vertical conductors (for instance, vertical-sheet massive sulfide deposits or vertical/subvertical water-filled faults oriented perpendicular and parallel to the flightpath respectively). The *z*-axis (transmitter and receiver both having vertical-axis co-planar) component signal is optimally coupled for measuring the conductivity of horizontal layers beneath the ground surface. This

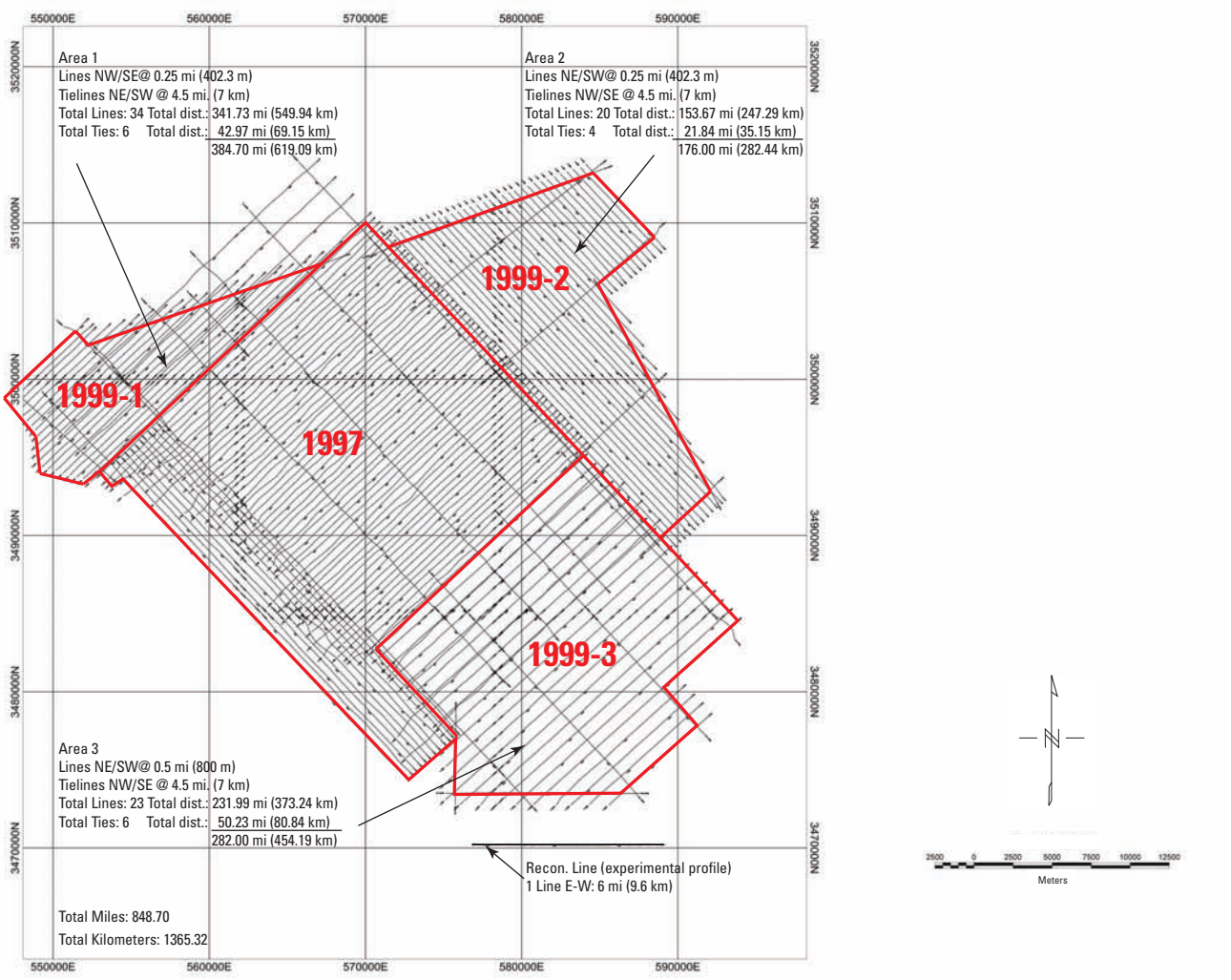

1999 Tombstone airborne geophysical survey (Geoterrex-Dighem, 1999)

Figure 3. Map showing survey lines and survey parameters for the three 1999 Tombstone airborne geophysical survey segments adjacent to the survey lines from 1997. Data from Geoterrex-Dighem (1997, 1999). Total distance figures include 10-kilometer-long experimental profile (see p. 26 and pl. 2).

coil orientation was found in this study to be the most useful for mapping shallow horizontal conductors, such as conductive ground water. All three components will report anomalies over powerlines, pipelines, and grounded fences. The transmitter, by virtue of its horizontal layout, is geometrically configured to induce (primarily) horizontal-plane eddy currents in the ground; the vertical (z-axis co-planar) receiver coil is thus optimally coupled to detect a secondary field from these eddy currents as deep as 400 meters.

The GEOTEM-transmitted waveform is a unique half-sine-wave-followed-by-an-off-period signal that can be lengthened for maximum penetration depth or shortened for maximum near-surface resolution. For this survey, the waveform was lengthened to near its maximum for the deepest possible penetration; that is, a 30-hertz repeat rate and a 4-millisecond sampling rate. The output channels consisted of sampling windows taken at increasing time gates (which could be translated as correlating with increasing depth below the surface) in the received secondary waveform for each of three coil orientations. In addition to 60 EM channels (20 time windows each, times the three orientations, with an in-phase and a quadrature component for each channel), the GEOTEM system acquired data from a separate magnetic sensor, plus an additional 60-hertz monitoring channel to help distinguish manmade, grounded metallic structure anomalies (such as pipelines and powerlines) from geologic anomalies. These signals were location corrected during postflight data processing for the distance lag caused by the retarded position of the two detector birds trailing behind the aircraft on their respective cables.

The GEOTEM system also acquired Differential Global Positioning System (DGPS) location signals, as well as continuous videotape of the ground (to resolve any remaining manmade-vs.-geologic-source issues and to use as backup to the DGPS location information). The DGPS reference beacon was located at the Sierra Vista Airport during the survey. The EM channels were calibrated periodically by flying over a

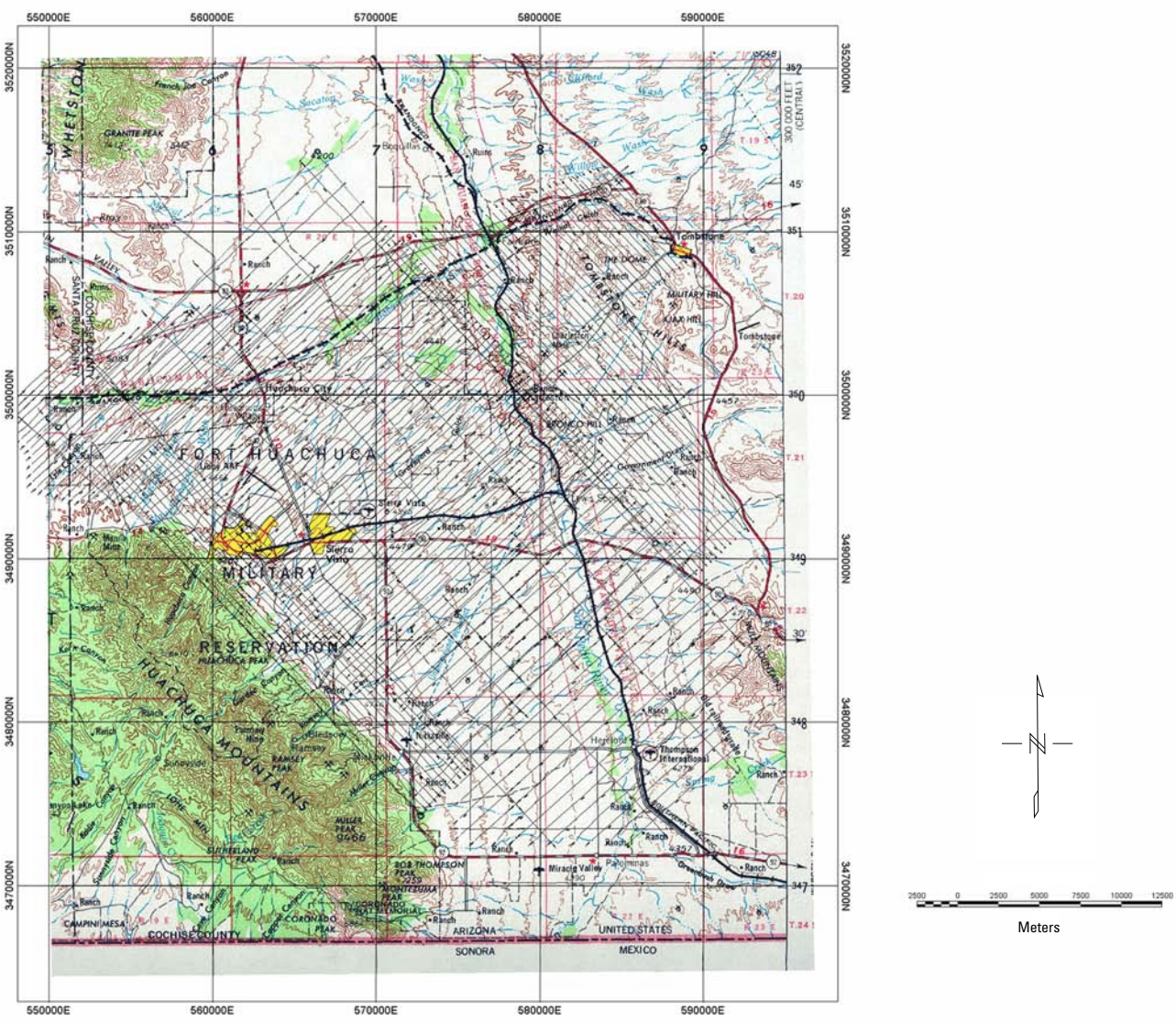

Base from U.S. Geological Survey 1:250,000-scale topographic map series. UTM zone 12. Data superimposed from 1999 Tombstone airborne geophysical survey (Geoterrex-Dighem, 1999).

Figure 4. Combined 1997 and 1999 aircraft survey lines superimposed on a topographic map of the Fort Huachuca area, Arizona.

well-characterized homogeneous target such as seawater and were also calibrated daily by flying the aircraft at the beginning and end of each survey at approximately 2,500 meters above ground level (AGL), so that any possible conductors were well beyond the reach of the rapid-fall-off dipolar transmitted signal, thus making ground contribution negligible. The data were also corrected for any residual signal caused by interaction of the transmitted pulse with the body of the aircraft (this correction is called "compensation"). Barometric elevation and radar-altimetry channels were also acquired to verify the vertical position of the aircraft.

Because the transmitted signal from an alternating electromagnetic dipole such as the GEOTEM transmitter antenna falls off rapidly as 1 over the distance cubed, it is critical to maintain the aircraft as close as possible to the ground for maximum signal penetration. During the 1997 San Pedro and 1999 Tombstone surveys, the aircraft was "drape-flown" over the terrain at about 125 meters AGL, with the exception of a zone flown at 155 meters AGL over populated areas such as the city of Sierra Vista and Fort Huachuca. This local exception was necessary to conform with Federal Aviation Administration (FAA) regulations. While flying at 125 meters AGL, the magnetometer was nominally about 40 meters below the aircraft, and the EM bird was slightly more than 50 meters below the aircraft.

The GEOTEM system is a time-domain EM system; that is, data were sampled at certain defined time gates, some before but most after the transmitter signal was switched off.

These time gates were sampled for each of the three components of the received EM signal detected at the towed bird. The base frequency was 30 hertz (the transmitter was switched on and then off again 30 times per second). The channels used to sample the received signal are listed in table 1. In this table, the delays indicate the start of the gated window in microseconds from the end of the transmitted pulse for the given channel. Negative delays indicate that the window was started before the end of the transmitted pulse; this method was used to gather sufficient information to calculate inversions of conductivity vs. depth.

Between the 1997 and 1999 surveys, the GEOTEM system was modified slightly; primarily, the channel designations were reordered in a more logical numerical sequence. To spline data blocks from both surveys, it was necessary to use the same time gates so the system was measuring approximately the same conductivity at the same depth. Because the transmitter set up eddy currents in any conductors in the ground, the secondary signal received (that is, the signal received at the towed bird after the primary transmitter signal was turned off) from deeper depths arrived later than a secondary response from shallower depths. Because an averaging effect was going on also, there was no direct linear relation between gate times and depths. As a rule of thumb, however, the longer the time delay in the sample gate, the deeper the detected source. For this reason, different time gates can be used to effectively sample different depths. Table 2 lists the correlation between the sampled channels of the 1997 and 1999 surveys. These channel equivalencies are presented with their relative depth of penetration indicated. Note that depth of penetration varies significantly over the target area and is controlled by variables such as aircraft elevation (increased flying elevation decreases depth penetration), degree of electrical interference (greater electrical interference reduces the signal-to-noise ratio and thus reduces depth of effective penetration), and ground resistivity (the greater the resistivity, the greater the depth of penetration). The CDT inversions discussed below compensate for most of the fluctuations in elevation.

Finally, by using the Geosoft Grid Knit software, the original 1997 dataset and the three 1999 datasets for the magnetic field, as well as the three EM channel grids, were spliced together. The splicing was seamless for the magnetic data and generally excellent for the EM channels, except for an imperfect splice made difficult by an area of high topographic relief in the Tombstone Hills in Area 2.

Table 1. Electromagnetic time-domain gates in the 1999 airborne electromagnetic survey.

[Data from Geoterrex-Dighem 1999]

Channel number	Window starting-point (delay in microseconds from the end of the transmitted pulse)
1	[1]-3,906
2	[1]-3,169
3	[1]-1,975
4	[1]-782
5	[1]-44
6	195
7	391
8	630
9	911
10	1,215
11	1,541
12	1,931
13	2,409
14	2,995
15	3,733
16	4,665
17	5,837
18	7,313
19	9,136
20	11,306

[1]Transmitter-on data are important to precisely characterize the transmitted signal.

Quality Control Analysis

The GEOTEM airborne geophysical system is advanced and complex, and as a result there are many variables that can affect data quality. These variables include the relative locations of the towed birds with respect to the aircraft. The dipolar nature of the transmitted signal means that there are significant changes in detected signal strength for only small

Table 2. Channel equivalencies between the 1997 and 1999 airborne electromagnetic (AEM) surveys.

1997 AEM survey channel number	1999 AEM survey channel number	Relative depth penetration
2	10	Shallow
6	14	Intermediate
10	18	Deep

changes in geometry—even if absolute coil-to-coil separation is unchanged. The relative position of the birds has been shown to have a significant effect on the data, both in signal strength (fluctuations can thus look like changes in subsurface resistivity) and signal-to-noise (the noise threshold can exceed the signal, especially for secondary signals from deeper conductors). If the aircraft moves up and down significantly while draping rough terrain, then the system will detect apparent fluctuations in resistivity (there is a lesser, but still non-zero, effect of these fluctuations on the magnetic data). Extensive engineering work has gone into compensating for this elevation-fluctuation effect, but procedures to correct for these inevitable fluctuations can never be perfect. The GEOTEM system was designed, however, to hold these signal-strength fluctuation effects to the part-per-million range for most flying conditions.

In addition to structural flex in the aircraft-bird geometry, there can be short-wavelength errors in the radar altimetry data (from electrical interference such as regional lightning or airport radar transmissions) and long-wavelength errors in barometric altimetry data (from weather systems moving through the area), both of which affect the signal strength and thus the apparent resistivity of the local subsurface sediments. There is also the theoretical potential for temperature-controlled or vibration-caused changes in the GEOTEM electronic systems. Much of the work done by flight engineers and postprocessing technicians focuses on compensating for these potential errors.

The survey target areas, especially Area 2, have significant topographic relief that the aircraft must try to drape over. In addition, there is always some degree of air turbulence due to rising heat from the desert floor, especially in the afternoons. Twice during the 1999 survey, the aircraft was forced to return to base early when turbulence began to affect data quality. To check these various effects on the data finally reported by the contractor, the author generated several comparison figures.

The contractor carried out altimeter calibration by making a series of level overflights over the Sierra Vista Airport runway, whose elevation is well known. Results of these calibration flights are presented in figure 5, which shows barometric elevation fluctuations of less than 15 feet (less than 5 meters). The GPS elevation noise is also shown in this figure for comparison. Because GPS systems cannot take advantage of satellite geometry both above and below the aircraft (the Earth is in the way), the GPS elevations are always much noisier than the horizontal position. Therefore, the GPS elevations were not used in the survey except as a rough quality check.

Figure 6 shows a superposition of measured radar altimeter variations (in color) on shaded-relief topography (digital USGS elevation data in gray tones), with contour lines of the shallow (1999 EM channel 10) *z*-axis conductivity. In this figure, we can see the correlation between flightline directions, as well as topographic relief and the radar altimetry. Subtle fluctuations in the contours of the conductivity correlate closely with the slight "herringbone" effect in the radar altimetry. These fluctuations are all within contract specifications (some

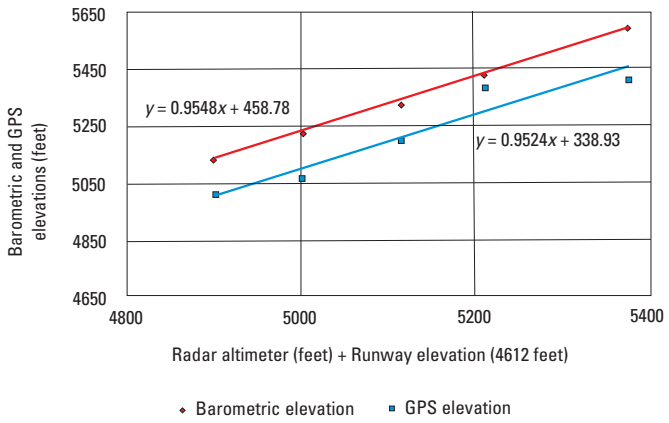

Figure 5. Graph showing altimeter calibration for the 1999 airborne geophysical survey. Calibration was based on a series of overflights made at the Sierra Vista Airport, Arizona. The GPS (Global Positioning System) elevation noise is also shown for comparison. Data from Geoterrex-Dighem (1999).

lines were reflown when the fluctuations exceeded contract specifications). In the 1997 survey, some of the coverage over occupied areas such as Fort Huachuca and Sierra Vista had to be flown at 155-meter terrain clearance because of FAA flight rules; uninhabited areas in the 1997 and 1999 surveys were overflown at an optimal terrain clearance of 125 meters to maximize penetration of the EM transmitted signal, while minimizing risk to the aircraft.

Figure 7 shows the radar altimeter variations (this time as contour lines) superimposed on the 1999 EM channel 10 *z*-axis conductivity (in color). Both are laid over shaded-relief topography (digital USGS elevation data in gray tones) for reference. This figure shows much more clearly that subtle wiggles on the edges of the conductivity anomalies in Area 2 are caused by radar altimeter fluctuations, which in turn are caused by the aircraft attempting to drape some of the more rugged topography. This figure also shows that the effects of uncompensated aircraft motion are relatively small, especially considering the nonflat topography of the target area.

Finally, figure 8 shows the radar altimetry fluctuations (in color) superimposed on the contoured shaded-relief topography. From this view it is clear that the fluctuations are almost all due to changes in the topography that the aircraft is attempting to negotiate. See, for example, the western parts of the Babocomari River (located around UTM coordinates 3500000N and 550000E to 555000E), where topographic relief caused larger than average variations in radar altimetry. Figures 3–8 indicate that the data returned by the contractor met (and generally exceeded) the survey contract specifications.

These comparisons are self-consistency checks based on data released by the contractor. During the 1999 survey, the author served onsite as the contracting officer's representative, working with flight engineers and the data-reduction team to assure that quality-control procedures were strictly adhered to.

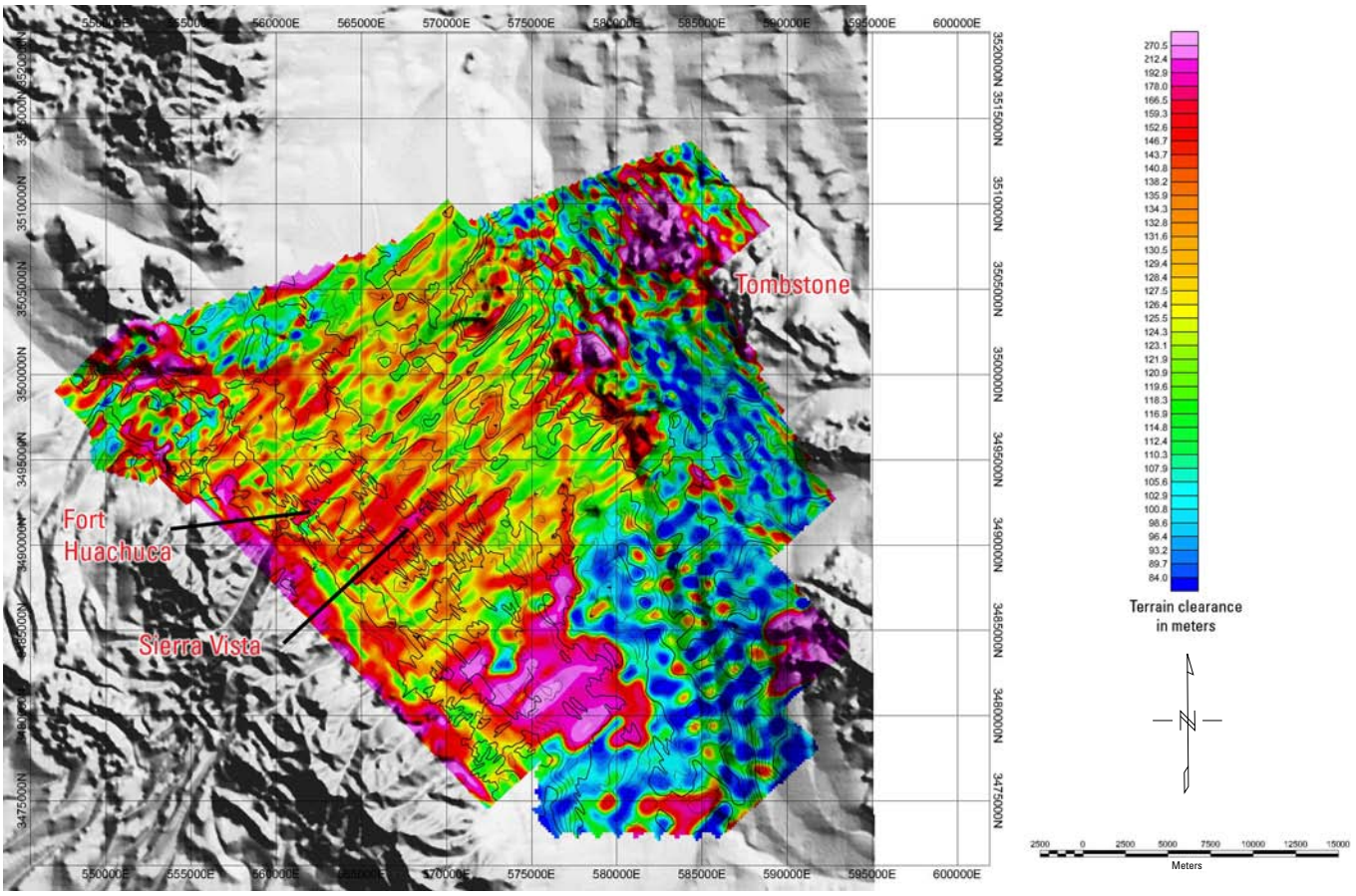

Base derived from U.S. Geological Survey Digital Elevation Model.

Figure 6. Measured radar altimeter variations (in color) superimposed on a shaded-relief topographic map of the Fort Huachuca area, Arizona (digital USGS elevation data in gray tones), with contour lines of the 1999 EM channel 10 (*z*-axis) conductivity.

The 1997 data have already been released separately (Bultman, Gettings, and Wynn, 1999).

Magnetic Data and Depth-to-Basement

Figure 9 shows merged magnetic data from the 1997 San Pedro and 1999 Tombstone airborne surveys for the Fort Huachuca area; the data are plotted in color and as contour lines and imposed on a UTM grid of the area. In the center, the data are dominated by a large magnetic high caused by the Tombstone volcanic field. In addition, the data show small magnetic-noise anomalies caused by Fort Huachuca and Sierra Vista. In the northwest, there is a magnetic high thought to be caused by Tertiary volcanic rocks. Only small volcanic outcrops are observed on the surface in the northwestern part of the survey area (Sean Kneale and others, U.S. Forest Service, written commun., 1997), and most of the mapped volcanic rocks are beyond the area shown in figure 9, to the north and northwest. The anomaly in the northwest implies that a significant amount of Tertiary volcanic material underlies the Tertiary-Quaternary sediments near Huachuca City (Tv outcrops in several places north of Fort Huachuca in front of the Mustang Mountains and along the Babocomari River; see Drewes, 1980). The data in figure 9 are not particularly useful unless we have an interest in the geology of the volcanic rocks or the basement rocks, subjects beyond the scope of this report. Magnetic contour maps generally show relatively little of the total information available in the magnetic data from which they are contoured. In this case, the strong magnetic high from the Tombstone volcanic field overshadows the remaining dataset.

We can extract additional information hidden in subtle variations in the magnetic data to provide depth-to-magnetic-source information. Wherever a small lateral change in the magnetic field strength occurs (in most cases, changes that are smaller than the contour intervals on these maps), we can calculate the depth to that source—presumably from a geologic contact between two different lithologies having slightly different magnetic-mineral (usually magnetite) content. Typically, geologic and fault contacts in crystalline basement rocks beneath a basin such as this cause these changes. However, with the presence of nearby Tertiary volcanic rocks (Drewes, 1980; Gettings and Houser, 2000), we must consider the possibility that there are volcanic flows intercalated in the sediments above the crystalline basement.

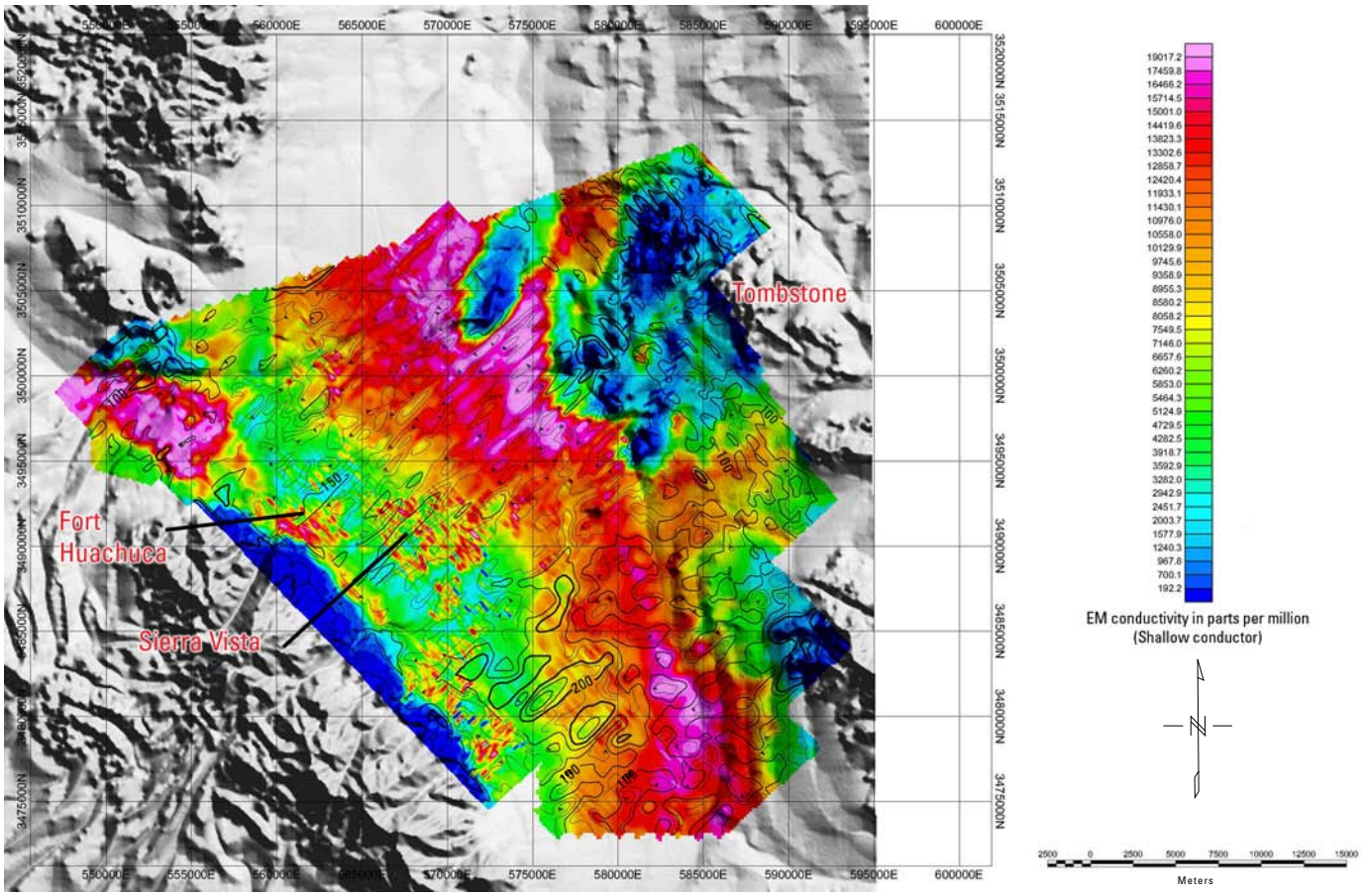

Base derived from U.S. Geological Survey Digital Elevation Model.

Figure 7. Radar altimeter variations (as contour lines) superimposed on the 1999 EM channel 10 (*z*-axis) conductivity (in color), over a shaded-relief topographic map of the Fort Huachuca area, Arizona (digital USGS elevation data in gray tones). Altimeter variations were small; contours labeled 100 indicate a deviance of 1.00 meter from the target elevation.

One method for calculating depth-to-source from magnetic data is Euler deconvolution (Reid and others, 1990; Blakeley, 1995). In an area having many subtle variations in magnetic field strength (each caused by a change in magnetite content in the underlying lithology), a model can be constructed that breaks the anomaly source into many small prism-shaped sources. An analytic model that calculates the effect of each simple prism-shaped source can be incorporated into an "inversion" system; that is, an algorithm that continually compares the aggregate model solutions for a segment of the magnetic map and modifies the model source until it obtains a "best fit." In fact, the inversion effort (that is, going backward from the magnetic data to the geologic source) is best carried out as a nonlinear process, as experience has shown that the comparison and modification part of the process can quickly become unstable. If the algorithm thus developed is passed along a profile, then the algorithm can calculate depth-to-source for multiple sources very quickly. Because these results vary widely in quality (depending on the noise in the original data), they must be "windowed" (that is, selected for sensitivity of the result to slight variations in horizontal and vertical changes in the small prism model sources).

Euler deconvolution was carried out on the merged 1997/1999 magnetic dataset. The results can be represented in several different ways, each of which has advantages and disadvantages. Figure 10 depicts Euler deconvolution solutions (shown as circles) superimposed on a topographic map of the upper San Pedro drainage. Each of the numerous circles represents a windowed (acceptable quality or low-noise) solution for a small change in the magnetic field strength; circles having warmer colors indicate a deeper source. This graphic presentation allows the geophysicist to see both the quality of the data (by the coherence of the solution circles) and—equally important—areas where data are scarce (by the absence of solution circles in low-gradient zones). In addition, structural information can be gleaned from this type of presentation. Circles that lie along a line represent either a geologic contact or a fault-offset in the crystalline basement. They can also represent geologic contacts between nonmagnetic sediments and thin layers of magnetic volcanic rock interleaved within the sediments. Finally, stacked but offset circles imply a dip or tilt in the horizontal plane in the geologic or fault contact.

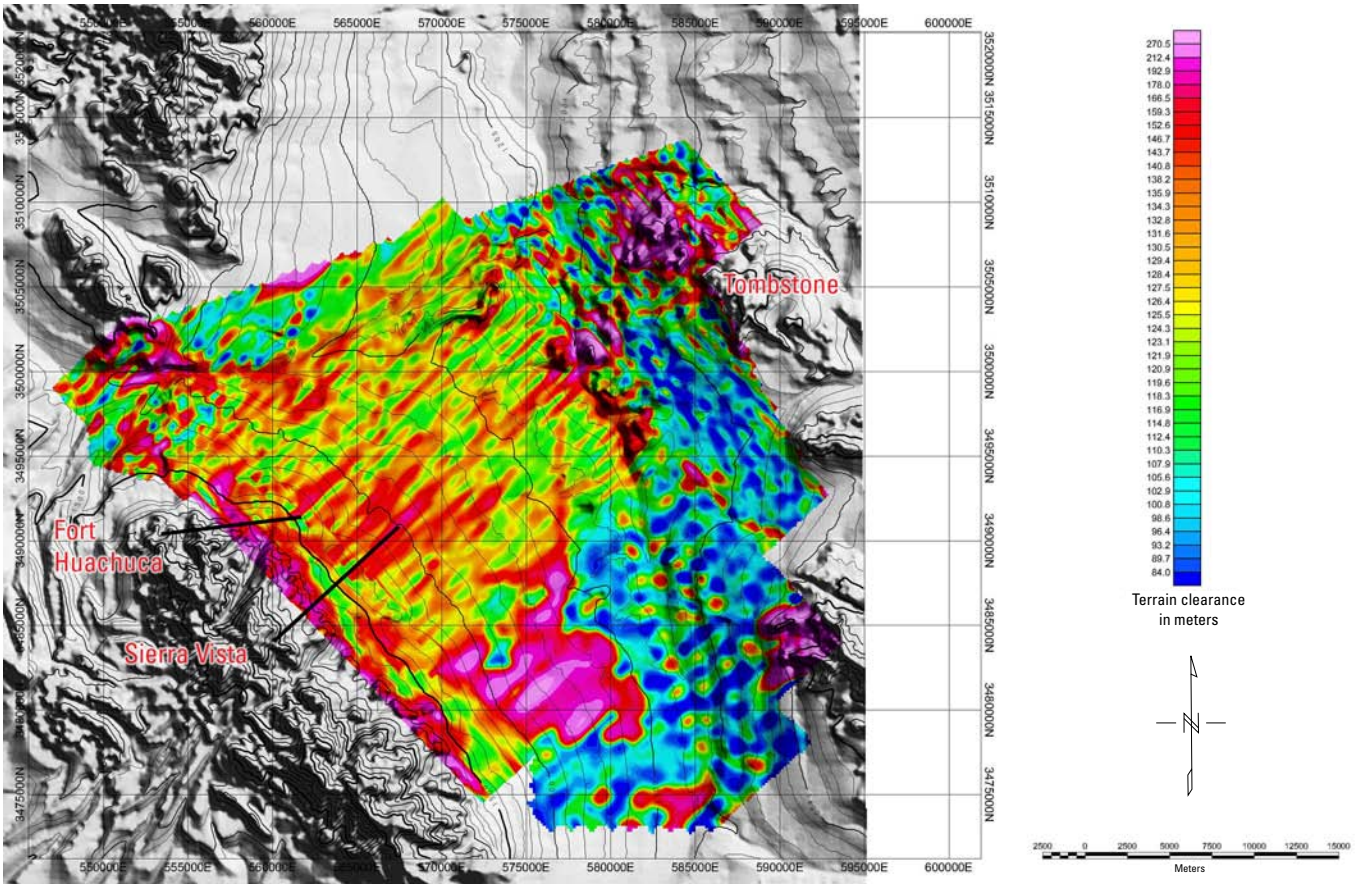

Base derived from U.S. Geological Survey Digital Elevation Model; contours in meters.

Figure 8. Radar altimeter variations (in color) superimposed on a contoured (for clarity) shaded-relief topographic map of the Fort Huachuca area, Arizona (digital USGS elevation data in gray tones).

We can also present the results of the magnetic depth-to-source calculations by using colors, as shown in figure 11. Cooler colors in this depth-to-source map represent deeper basement, and warmer colors represent shallower basement. For reference, figure 12 shows the contours of depth-to-basement derived from gravity data (Gettings and Houser, 2000). The gravity contours are based on a much sparser gravity station dataset. The magnetic data show a much more complex basement than the gravity map in figure 12 shows. Most of the differences can be ascribed either to the greater density of magnetic data or to geologic noise. Geologic noise has many causes; one example is different depth solutions caused by magnetic rocks lying at two different depths, one over the other.

Near Huachuca City, there is an apparent ridge in the basement that is almost certainly caused by a narrow channel filled with volcanic material from the Tertiary volcanic rocks that are now intercalated in the sediment stack in the northwestern part of the survey area. This apparent ridge is located at UTM coordinates 3500000N, 564000E in figure 11.

The San Pedro River, with one or two small exceptions in the study area, runs over parts of the basin underlain by shallow crystalline rock and relatively little sediment. The electrically conductive aquifer (discussed on p. 17 and 18) correlates well with the deeper sections of the basement lying to the west of the river. In the northeastern quadrant of the study area, the San Pedro River, Walnut Gulch, and the Babocomari River intersect and are underlain by large sections of shallowly buried to surficial exposures of the Tombstone volcanic field. The relation between the basin sediments and the bedrock in the Tombstone Hills area is complex and may be both stratigraphic (Cenozoic basin sediments unconformably overlie the Cretaceous intercalated volcanic flows in the sedimentary stack) and fault bounded. This region lies within the mapped Tombstone caldera margin (Moore, 1993). Also in figure 11, one can see a roughly east-west deep basement feature (the blue feature extending from the right to about UTM coordinates 3495000N, 580000E in the middle) south of Tombstone that apparently intersects another northwest-southeast deep basement zone roughly paralleling the Huachuca Mountain front but lying to the east of it (the NNW-SSE blue zone at the left-center of figure 11).

The magnetic depth-to-source map in figure 11 agrees remarkably well with the gravity depth-to-basement map

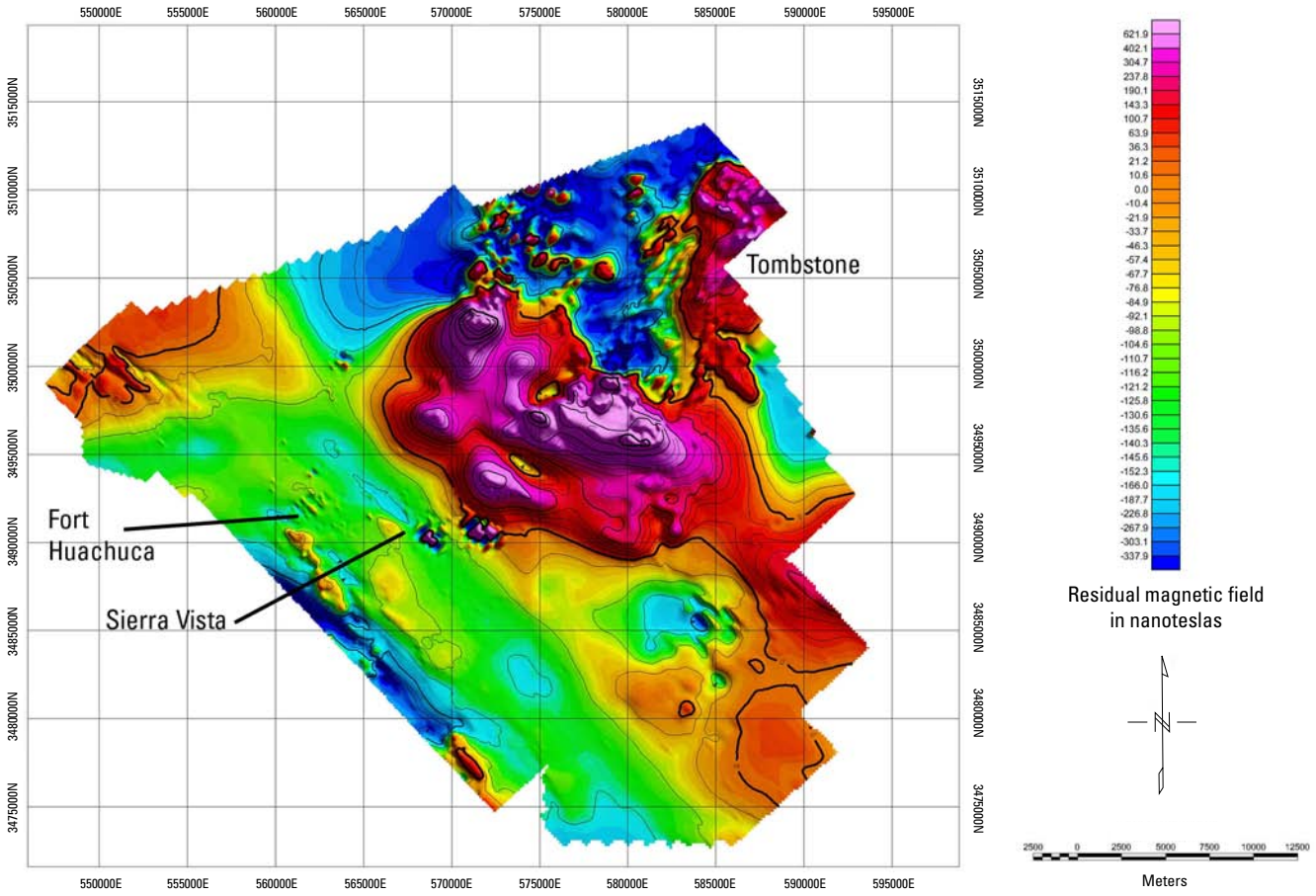

Base derived from U.S. Geological Survey Digital Elevation Model.

Figure 9. Aeromagnetic data map showing merged magnetic data from the 1997 San Pedro and 1999 Tombstone airborne geophysical surveys for the Fort Huachuca area, Arizona. Data are depicted in color and as contours and show a large magnetic high caused by the Tombstone volcanic field, as well as several smaller magnetic anomalies. Data are plotted on a Universal Transverse Mercator grid of the area.

(fig. 12). A structural high (probably a horst or uplifted fault-block) underlies the city of Sierra Vista centered around UTM coordinates 3490000N, 570000E. A driller's log of well D(21-20)35abb, which encountered crystalline basement at 237 meters beneath the city, verifies this feature. A north-south fault (roughly along UTM longitude line 565000E) also extends from the Whetstone Mountains (which lie just beyond the northwest corner of the study area) to the Huachuca Mountains on the south (referred to in Gettings and Houser, 2000, as the "Range-Front Fault"). The deep (at least 1,000 meters) basin beneath Huachuca City (UTM coordinates 3505000N, 562000E) appears in figure 11 to be more than one basin. The apparent ridge in the middle, however, is likely a stringer of volcanic materials in the middle levels of the sediment stack from the Tertiary volcanic rocks that lie just off the northwestern corner of the map and tiny outcrops in the Babocomari River (Gettings and Houser, 2000). The magnetic depth-to-source map suggests east-west faulting and uplift of basement rocks, probably related to 16-million- to 20-million-year-old Basin-and-Range faulting, though an east-west orientation is unusual in such faulting. There is some geologic evidence that these faults have been recently active (Gettings and Houser, 2000). This map and geologic mapping to the north of the study area (Gettings and Houser, 2000) seem to indicate north-south faulting of an indeterminate character.

The results obtained from the Euler deconvolution of the magnetic data should enable hydrologists to better assess the thickness of the upper San Pedro drainage sediments that lie deeper than the airborne electromagnetic system can penetrate. Depending on the degree of human electrical cultural interference present locally, the maximum direct depth of water detection by the GEOTEM Airborne ElectroMagnetic System

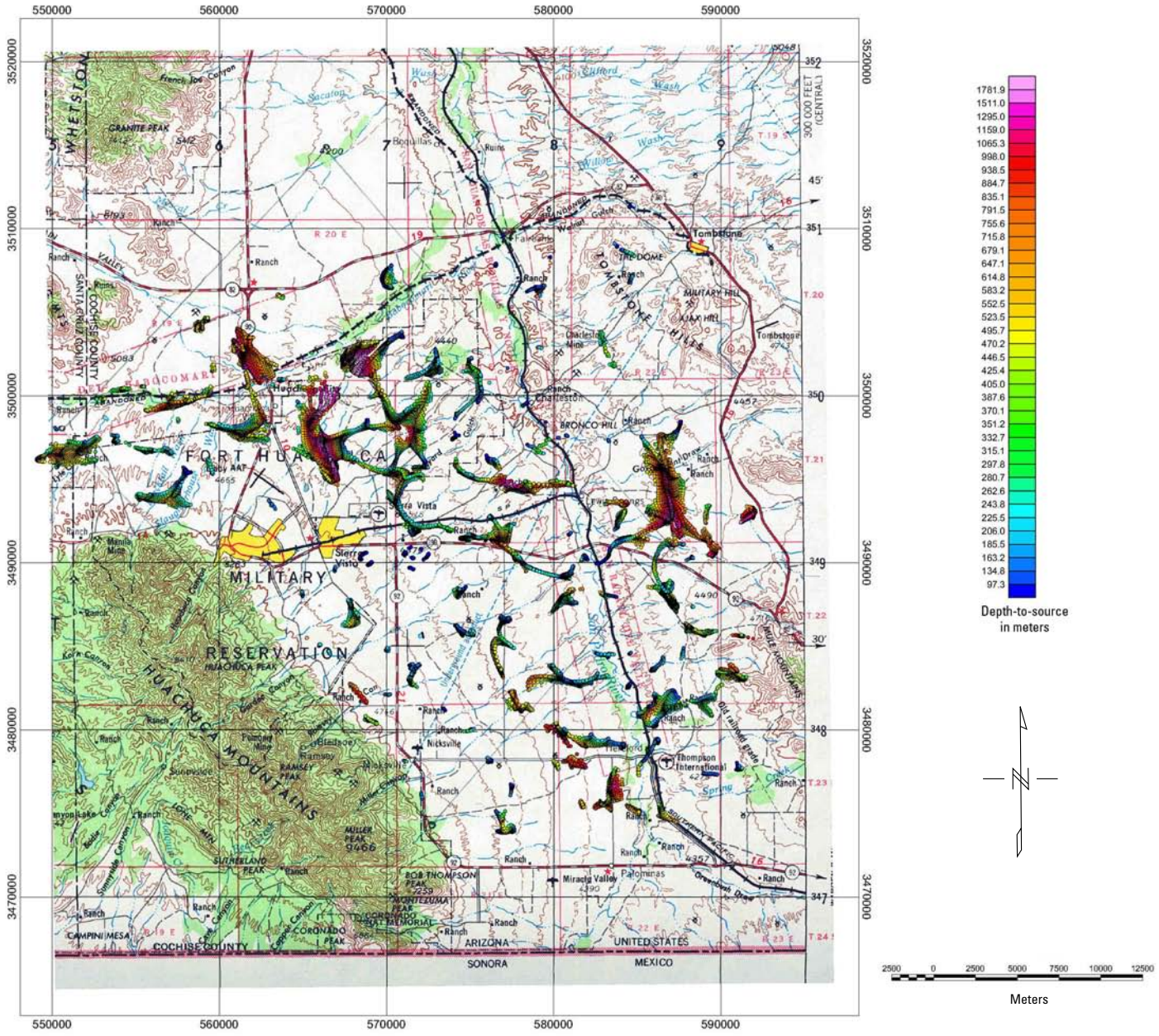

Base from U.S. Geological Survey 1:250,000-scale topographic map series.

Figure 10. Euler deconvolution solutions superimposed on a topographic map of the Fort Huachuca area, Arizona. The colors of the solution circles correlate with depth to magnetic basement; warmer colors indicate deeper sources. The locations of individual solutions show magnetic gradients that are generally geologic contacts or faults in the crystalline basement rocks.

(discussed in the following section) could be anywhere from 100 to 400 meters. However, structures deeper than 300 to 400 meters are of little hydrologic significance because there is generally less ground-water flow with depth and the sediments at great depth have reduced porosity due to consolidation and compaction (Ingebritsen and Sanford, 1998, p. 274). The CDTs discussed below appear to support this condition by showing closure (termination) of many of the electrical conductors at depth.

The Airborne EM Data and Water in the San Pedro River Basin

Because they are so similar to the *z*-axis EM data analyzed in detail below, the *x*-axis and *y*-axis airborne EM data in the upper San Pedro River basin are not discussed here. Instead, the following interpretation focuses almost exclusively on the z-axis imagery because it is an optimally coupled

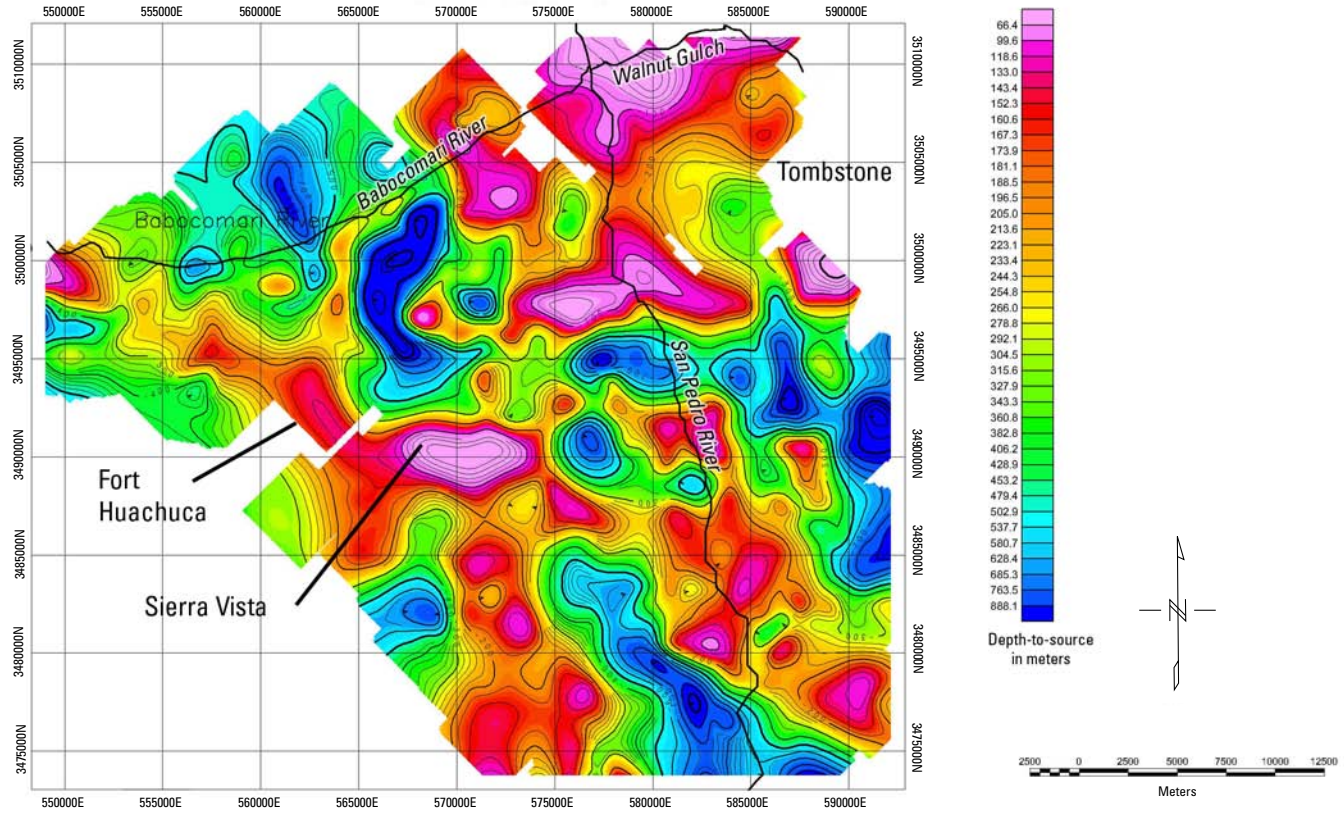

Base derived from U.S. Geological Survey Digital Elevation Model.

Figure 11. Map of the Fort Huachuca area, Arizona, showing magnetic depth-to-source data (crystalline basement in most cases) from Euler deconvolution of magnetic data (Hanning filtered for clarity) for a structural index of 0. The 0 index was chosen to emphasize step-offsets and geologic contacts. Note that in figure 10, warmer colors indicate deeper sources, whereas in this figure, warmer colors indicate shallower sources.

signal for mapping horizontal and subhorizontal conductors. This approach is just the opposite of that of airborne EM investigators searching for mineral resources, where complex vertical and subvertical structures are generally the key to understanding the mineralization process.

Figure 13 is a Thematic Mapper image of the Sierra Vista subbasin of the upper San Pedro River drainage; it was taken from a larger Landsat Thematic Mapper image by Dohrenwend and others (2001). The bright colors were deliberately enhanced to show subtle differences in surface rocks and soils that can be attributed to hydrothermal alteration, a process closely related to mineralization. The figure is used here, however, to provide a recent (1997) index of the growing population of Sierra Vista and surrounding areas. Airborne EM data are strongly influenced by human cultural interference such as powerlines and pipelines.

Figures 14, 15, and 16 show the airborne EM images acquired by using the *z*-axis coil in the GEOTEM system; they represent channel 10 (shallow), channel 14 (intermediate), and channel 18 (deep) data, respectively. The channels referenced here are from the 1999 survey, but the results apply to the 1997 area, as well. The redder or warmer colors represent zones of higher conductivity caused by the occurrence of water, with some additional contribution from clays. In these figures, lines represent the San Pedro River, the Babocomari River, and Walnut Gulch. These features were digitized from the U.S. Geological Survey 1:250,000-scale topographic map of the area.

The San Pedro basin lies in a relatively arid zone, and the ground water has a generally higher conductivity from less extensive flow-through than that in wetter, more temperate regions of the United States. Rainwater normally has very low conductivity, but when it rests in an aquifer over an extended period, it takes on dissolved ions from the surrounding rocks and soils and becomes more conductive, unless flushed by recharge and ground-water flow. Ground water in the San Pedro regional aquifer is potable and considered good quality in comparison with water in nearby arid basins (Pool and Coes, 1999). Conductance of ground water in the regional aquifer ranges from about 200 to 1,200 µS/cm and averages 338 µS/cm, which corresponds to a resistivity of 30 ohm-meters (values from Pool and Coes, 1999, pl. 3). Most geophysicists consider even 200 µS/cm to be conductive ground water (Ken Zonge, Zonge Engineering & Research, Tucson, Ariz., oral commun., 1999; also personal experience of the author). Slightly lower conductivity values in the Sierra Vista

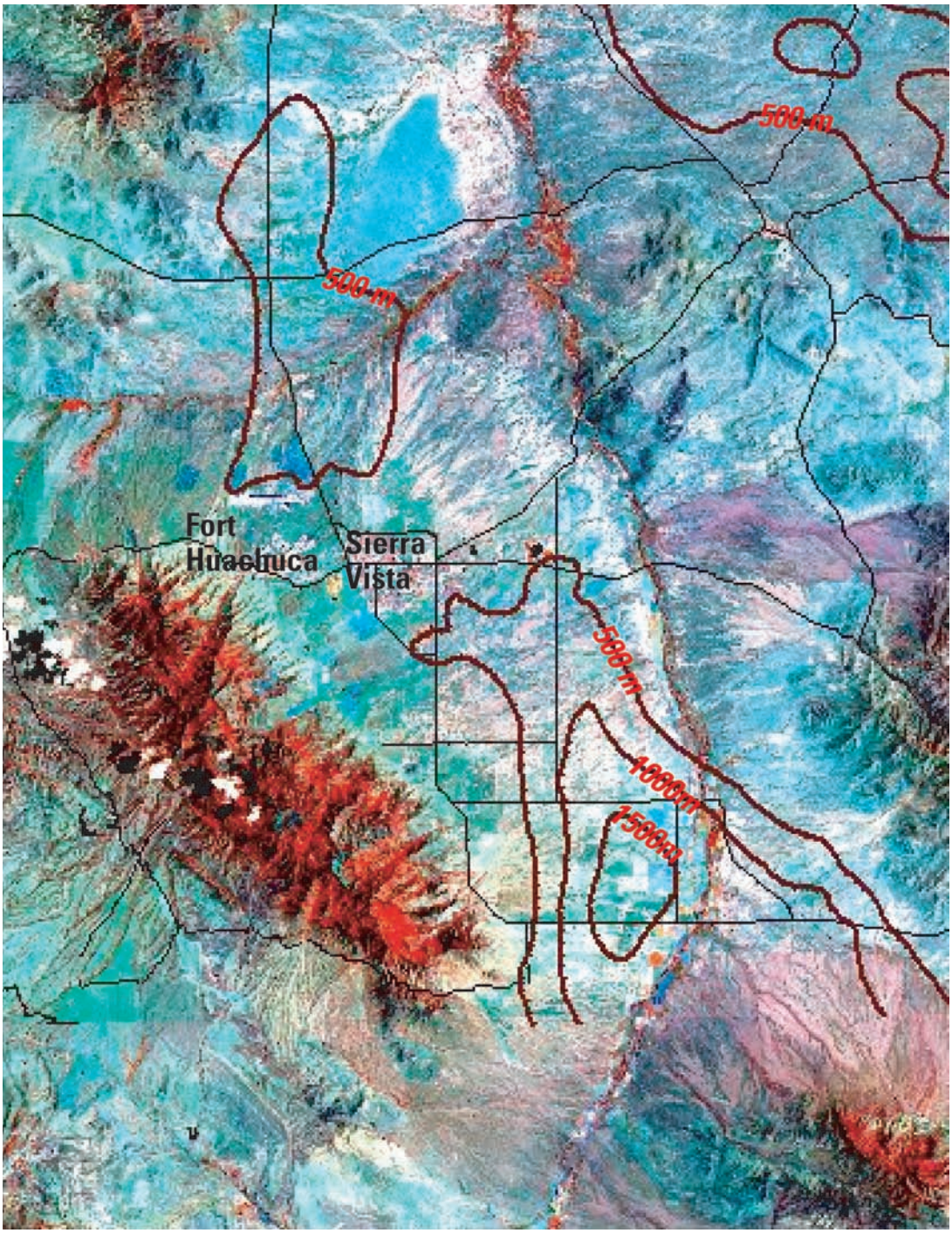

Base from Gettings and Houser, 2000.

Figure 12. Map of the Fort Huachuca area, Arizona, showing depth-to-basement data derived from modeling gravity data (Gettings and Houser, 2000); contours in meters (m). Compare with figure 11.

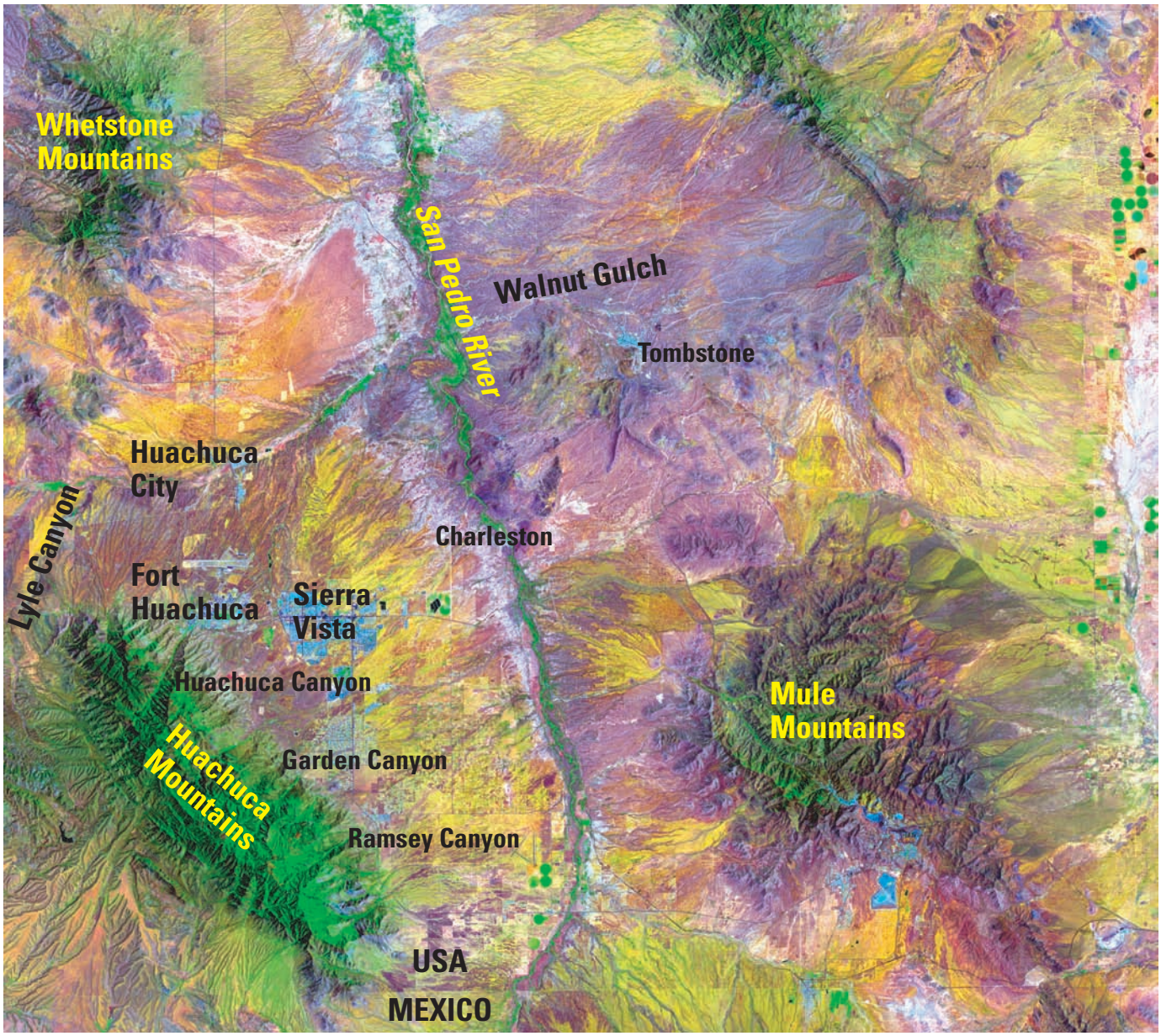

Landsat Thematic Mapper image from 1997.

Figure 13. Thematic Mapper image of the Sierra Vista subbasin of the upper San Pedro River drainage. Derived from Dohrenwend and others (2001), with key features labeled and colors enhanced. The light-purple zones immediately west of the San Pedro River correlate with significant vegetation and several springs.

subwatershed in comparison to those of the nearby Tucson basin (between 300 and 500 µS/cm) suggest a more recent age since time of recharge of the system. The presence of clays in the San Pedro basin may further enhance conductivity values, but conductivities of ground water in the basin are already quite high.

The most electrically conductive parts of the aquifer (more than 800 µS/cm conductance or less than 12.5 ohm-meters resistivity) probably correlate with saturated silts and clays and with conductive sediments detected in electrical well logs, particle size logs (wells TW1, TW3, TW5, TW8, TW9, and MW7), and several vertical electrical soundings used to define the extent of the fine-grained sediments in the Sierra Vista subbasin (Pool and Coes, 1999). Moderately electrically conductive sediments in the aquifer (200 to 800 µS/cm) generally correlate with saturated sand and gravel. Less conductive materials (less than 200 µS/cm) are generally non-aquifer materials such as crystalline rocks. Fine-grained parts of the Pantano Formation, a poor aquifer, and the Cretaceous Morita Formation, a mudstone deposit, can also be weakly to moderately electrically conductive if water saturated and can be confused with fine-grained parts of the aquifer. These

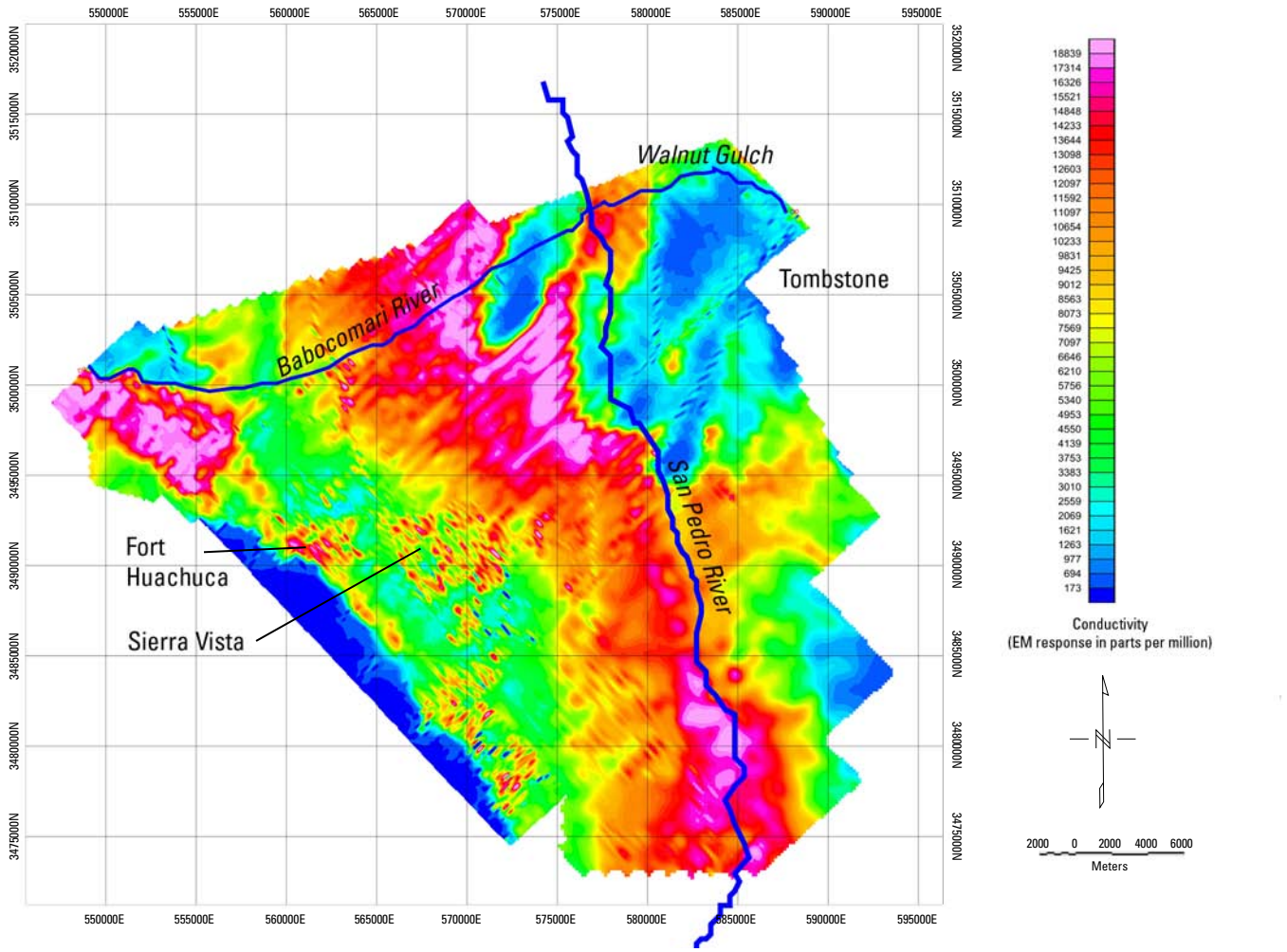

Base derived from U.S. Geological Survey Digital Elevation Model.

Figure 14. Map of the Fort Huachuca area, Arizona, showing combined results from the 1997 and 1999 airborne EM surveys, *z*-axis component (which emphasizes flat-lying electrical conductors), for channel 10. Because channel 10 is the shortest time gate, shallow electrical conductors are emphasized in the figure. "Speckling" indicates human electrical cultural noise (for example, powerlines and pipelines).

sediments are likely to occur in the near surface close to the Huachuca Mountains (Sean Kneale and others, U.S. Forest Service, written commun., 1997).

The clay-contribution-to-conductivity issue bears some discussion. On the basis of several hundred laboratory sample electrical measurements made while working for an engineering firm in Tucson, plus several hundred line-kilometers of resistivity/induced polarization surveys measured and interpreted in southeastern Arizona and other arid environments, the author believes that clays have a relatively minor effect on the already high conductivities observed in the AEM data in the San Pedro Valley. Clays may affect the amplitude of airborne EM conductors but not their horizontal or vertical location in the inversions. Further, the effect of clays is not particularly significant in areas like the San Pedro Valley where ground water is already so highly conductive (about 338 µS/cm or 30 ohm-meters resistivity on average and, in a few cases, above 800 µS/cm). Keller and Frischknecht (1966, p. 449) showed that, above about 5 percent clay content, cation exchange capacity becomes saturated. In other words, the contribution to conductivity from clays remains constant (and even declines) for clay content above 5 percent. In work in a similar arid environment in Saudi Arabia (Flanigan and Wynn, 1979), wadis were found to be conductive only down-drainage from mineral deposits, whereas the clay content was uniform along the entire length of the wadi. Thus, from the Huachuca Mountain front to the center of the basin, clays probably do not contribute significantly to the conductivity, no matter how much the clay content may increase. Consequently, the airborne geophysical data cannot reliably show the variation in clay content over the basin but can indicate where water is present. By inference, these data can also tell us something about the porosity of the sediments.

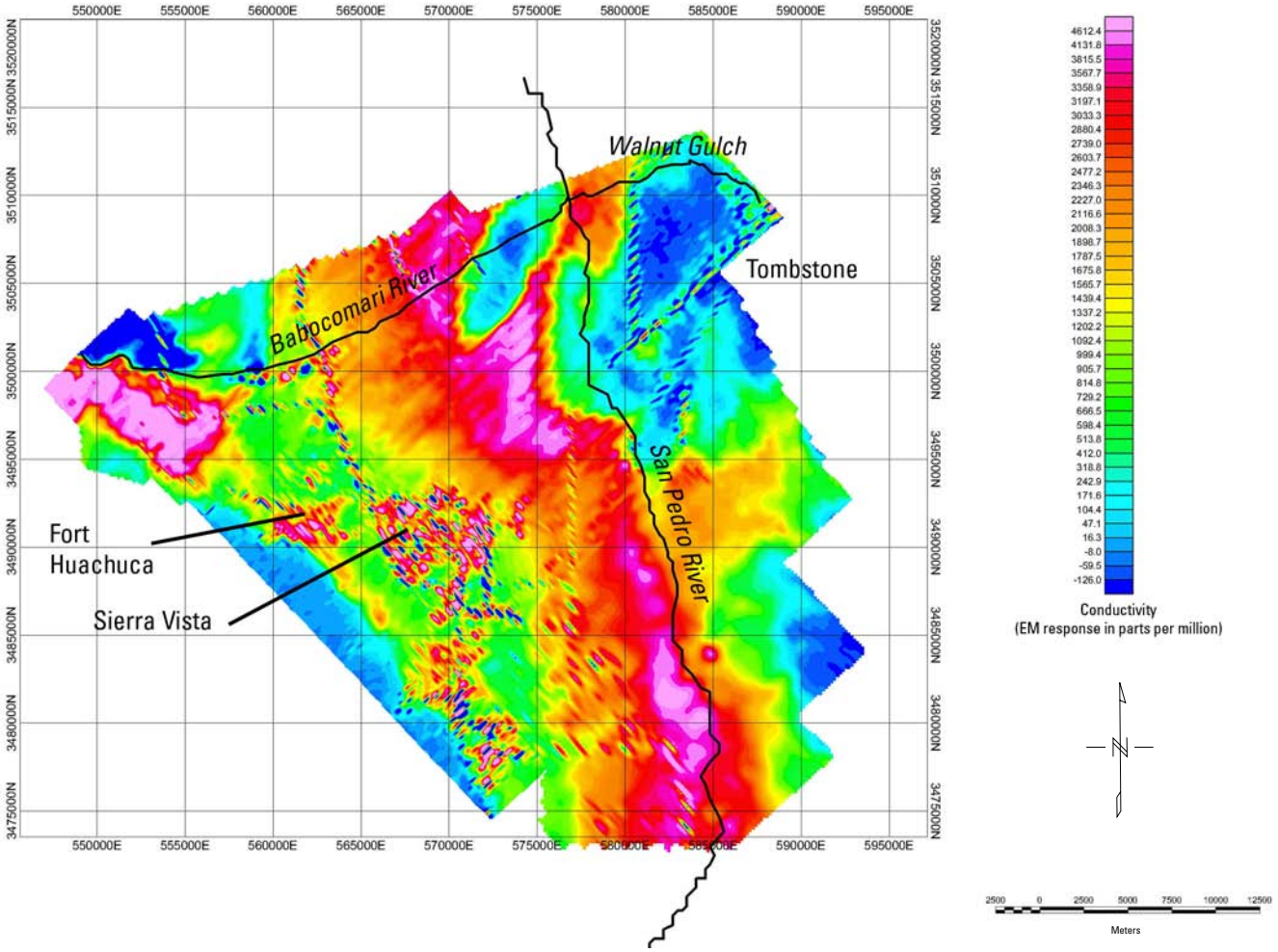

Base derived from U.S. Geological Survey Digital Elevation Model.

Figure 15. Map of the Fort Huachuca area, Arizona, showing combined results from the 1997 and 1999 airborne EM surveys, *z*-axis component (which emphasizes flat-lying electrical conductors), for channel 14. Because channel 14 is an intermediate time gate, intermediate-depth electrical conductors are emphasized in the figure. "Speckling" indicates human electrical cultural noise (for example, powerlines and pipelines).

Dark-blue areas in figures 14–16 correlate closely with the Tombstone volcanic field. These blue areas extend westward beyond where volcanic rocks appear on the geologic map by Moore (1993), indicating that the volcanic rocks extend under the more recent sediments westward of their geologic map location. The San Pedro River cuts through the Tombstone Hills volcanic rocks in the northern part of the survey area, and the AEM data clearly show that no significant shallow water is present beneath the river there. An extension of the large, central high-conductivity zone (red and purple areas in figures 14–16) through the Tombstone Hills correlates with a zone of denser vegetation north of Graveyard Gulch, roughly northwest of Charleston and east of Huachuca City, and extending into the western reaches of Walnut Gulch. Not surprisingly, the area where the Babocomari River and Walnut Gulch intersect the San Pedro River coincides with a zone of higher conductivity (red) that represents the southern end of another component of the regional aquifer lying north of the study area. A subtle offset in the warm colors in all three figures around UTM coordinates 3487000N and 575000E coincides with the Sawtooth Canyon fault of Drewes (1980, 1996). The geophysical data imply a left-lateral throw that geologic mapping by itself cannot show.

The speckling effect in figures 14–16 depicts human electrical cultural interference (from powerlines and pipelines). Figure 14 clearly shows that the speckled areas west of the main high-conductivity/low-resistivity zone correlate with the powerlines and pipelines above and beneath Fort Huachuca and Sierra Vista. Speckled zones in the south-southwest of the survey area correlate well with more recent extensions of human settlement to the south toward Garden Canyon and Ramsey Canyon.

Figure 16 shows much stronger interference in the survey area than figure 14 shows. This finding is counterintuitive,

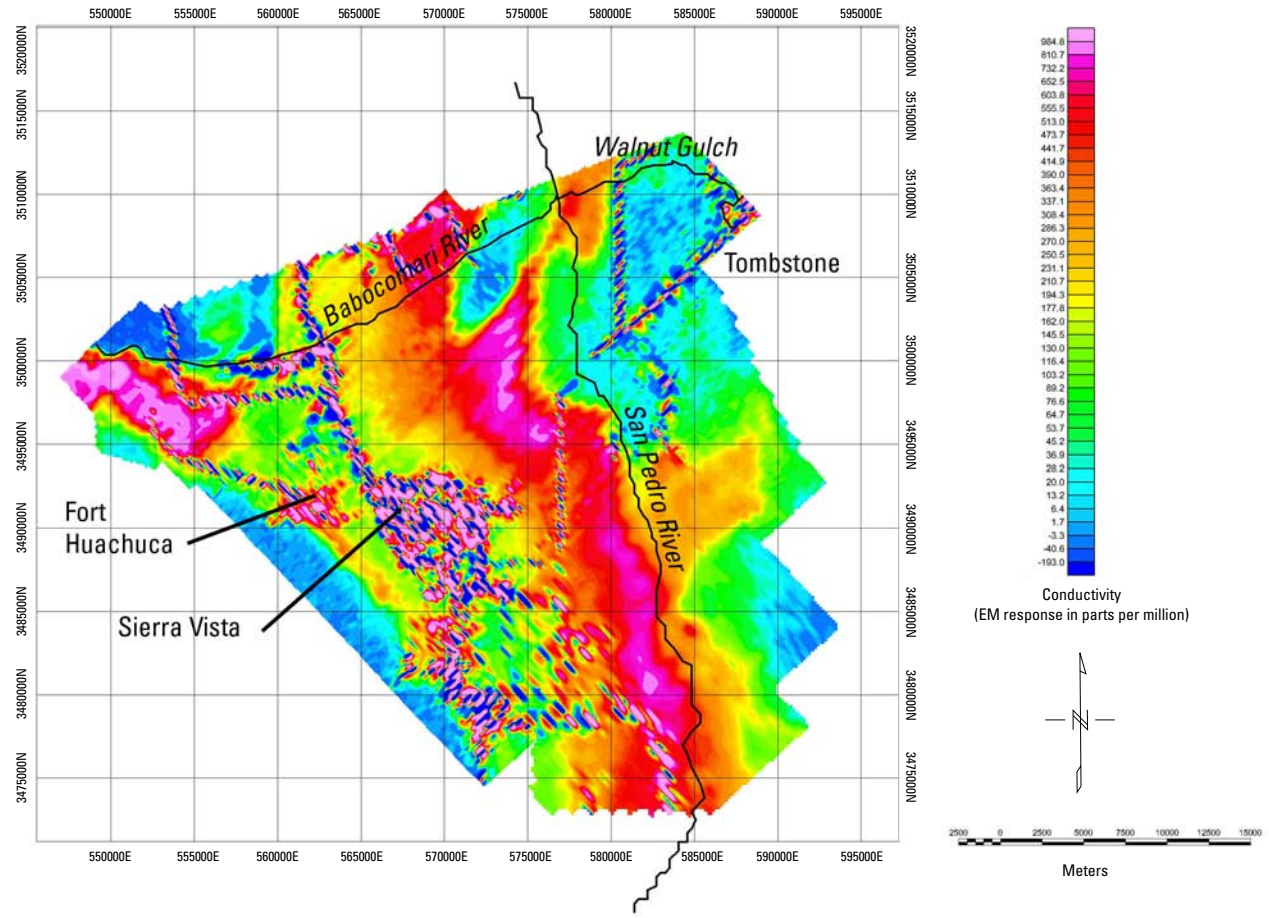

Base derived from U.S. Geological Survey Digital Elevation Model.

Figure 16. Map of the Fort Huachuca area, Arizona, showing combined results from the 1997 and 1999 airborne EM surveys, *z*-axis component (which emphasizes flat-lying electrical conductors), for channel 18. Because channel 18 is the longest time gate, deep electrical conductors are emphasized in the figure. "Speckling" indicates human electrical cultural noise (for example, powerlines and pipelines).

as figure 16 represents the output of EM channel 18 (*z*-axis), the most deeply penetrating EM channel. In fact, the deeper penetrating (or longer time lag) EM signals are attenuated more than the shallower signals by the overlying, conductive water-saturated layers. The gains must be adjusted upward to bring out the deeper signals, and as a result, the "speckling" or human cultural noise from the powerlines and pipelines is more strongly represented. Thus, even though the powerlines and pipelines are at the ground surface, they appear more strongly in the data representing the deeper conductive sources.

The large, high-amplitude high-conductivity zone in the extreme west of the survey area (figs. 14–16) suggests a western extension of the regional aquifer around Lyle Canyon and Turkey Creek, an area having mesquite bosques (woodlands) and springs (Brenda Houser, USGS, Tucson, Ariz., oral commun., March 16, 2000). This conductor is probably caused by water present in parts of the Pantano or Morita Formations or pre-Tertiary sedimentary rocks that crop out near the Huachuca Mountains and along the Babocomari River (Drewes, 1980; Sean Kneale and others, U.S. Forest Service, written commun., 1997). This conductivity anomaly can occur, however, only if water is present. In the author's experience with hundreds of laboratory resistivity measurements from samples throughout Arizona, dessicated clay-bearing samples are not conductive. If the clay-bearing samples are hydrated with distilled water, they become mildly to moderately conductive, but they must be saturated. The relatively high electrical conductivity of the ground water in the San Pedro drainage area (Pool and Coes, 1999, pl. 3) makes it clear that high-ion-content water dominates the conductivity anomaly observed here in the airborne geophysical surveys. This finding is especially true as porosity is usually higher in fine-grained sediments near the center of a valley (Driscoll, 1986, p. 67). This conductor should be investigated further to define its character and extent beyond the airborne survey boundaries.

Close to the Huachuca Mountain front (the dark-blue areas on the southwestern edge of figures 14–16), there appear to be some small electrical conductors (narrow fingers of red parallel to the mountain front) that may be small, shallow,

buried water outliers. Fragments of fine-grained Pantano Formation, in general overlain by sand and gravel basin fill, have been mapped in this area, and Pantano Formation also shows up in test wells. The Pantano is not a particularly good aquifer, however (Brown and others, 1966). These small electrical conductors in the Huachuca Mountain front area do not appear to correspond to any powerlines or pipelines, and so they must be caused by the presence of subsurface water.

Figures 14–16 are in effect depth slices of the regional conductor. They appear to suggest a mountain-front-paralleling gap between the small electrical conductors and the large conductor (interpreted as the regional aquifer) toward the east. This apparent gap is actually a thick, mountain-front-following unsaturated zone, as revealed in inverted conductivity vs. depth profiles (discussed in detail below) and water-table-depth data. The electrical conductor is continuous below this thick unsaturated zone between the narrow electrical conductors along the mountain front to the west and the large electrical conductor to the east. Well drawdown has been documented locally to a maximum of about 22 meters in the area near the Fort Huachuca East Gate well field, but elsewhere it is more typically less than 15 meters. Well drawdown becomes nearly insignificant at 3 meters near the San Pedro River (Pool and Coes, 1999).

Geologic mapping (Gettings and Houser, 2000) has shown that there is a listric fault tilting sedimentary rocks to the southwest along the Huachuca Mountain front. Called the Nicksville fault, it is probably related to Basin-and-Range faulting (Brenda Houser and Mark Gettings, USGS, Tucson, Ariz., oral commun., 1999). According to Don Pool (USGS, Tucson, Ariz., written commun., 2001), however, this fault may be early to mid-Miocene in age because listric faulting is not common in mid- to late Miocene Basin-and-Range deformation. This faulting has in effect downdropped the less hydraulically conductive Pantano Formation more in the southwest than in the northeast. However, the younger upper-basin-fill sand and gravel sediments are not tilted. This southwestern tilting may explain the thick, mountain-front-following sand-and-gravel zone, but not why it is unsaturated, nor why the electrical conductor, which apparently represents the presence of water, lies deep beneath it. Wells drilled into this unsaturated zone encounter water at depth, which then rises in the wells, as if it had been confined, to what is then recorded as a water table (Brenda Houser, USGS, Tucson, Ariz., oral commun., May 16, 2000). The underlying Pantano Formation is an older, pre-Basin-and-Range basin fill unit (Tertiary age) with deformed and tilted bedding. It has widely varying electrical properties (Pool and Coes, 1999) but is generally well consolidated. It is also a poor aquifer (Brown and others, 1966). There is probably some ground-water discharge from this area north to the Babocomari River near Huachuca City (Mark Gettings and Don Pool, USGS, Tucson, Ariz., oral commun., 1999).

Near the Huachuca Mountain front, there are significant variations among nearby wells in the thickness of unsaturated resistive sands and gravels (basin fill) overlying the Pantano Formation. These variations suggest block-faulting between the Huachuca Canyon fault and the Sawmill Canyon fault of Drewes (1980) around the mouth of Huachuca Canyon. Detailed examination of data in this area (Mark Bultman, USGS, Tucson, Ariz., oral commun., March 14, 2001) reveals differences between water-table and electrical-conductor depth of 10–20 meters in a narrow window near the mouth of Huachuca Canyon. These deviations are among the largest between the electrical conductor and the water table in the survey area. It is possible that these deviations are an artifact in the conductivity-depth-transform calculations (discussed in detail below), but they may also be due to seasonal variations in water recharge in this canyon-mouth area. The water-table data used in this report were acquired as much as several years before the airborne EM survey.

Examination of figures 14–16 shows an electrical conductor, interpreted here to be the regional aquifer, underlying (and therefore in hydraulic contact with) much of the San Pedro River. In the northern part of the study area (north of 3495000N), however, where the river passes over and through the western margins of the Tombstone volcanic field, there is little electrical conductivity that we associate with ground water in any of the airborne EM channels. Some of this area is covered with limestone, but according to the magnetic survey, this area has a thin veneer of materials underlain by volcanic rocks. The lack of an electrical conductor here implies that the aquifer discharges directly to the San Pedro River in at least the southern two-thirds of the survey area (south of 3495000N) but not in the northern third.

The Landsat image (fig. 13) supports Pool and Coes' (1999) observation that significant water is lost to evapotranspiration through local vegetation. The light-purple zones immediately west of the San Pedro River correlate with significant vegetation and several springs. These springs appear to be caused by relatively insignificant ground-water flow reaching the surface as water moves eastward above silt and clay layers in the basin fill unit. The water table between Fort Huachuca and the San Pedro River becomes increasingly shallow as it approaches the river (see fig. 17). The amount of discharge from these springs is very small, however, and cannot account for most of the ground-water flow from the aquifer. The perennial water seen in the eastern reaches of the Babocomari River in the northern part of the study area must come from the upper San Pedro aquifer.

Figure 17 (an enlarged version of this figure is presented as pl. 1 of this report) shows an overlay of water-table depths (numbers in black) onto shallow (1999 EM channel 10) conductivity data. The warm colors (zones of high conductivity) are inferred to represent water. The water-table data are from Maurice Tatlow (Arizona State Department of Water Resources, written commun., 1998; an edited version of Tatlow's data table can be found in appendix 1 of Bultman, Gettings, and Wynn, 1999). Well data can be accessed at http://www.azwater.gov/dwr/content/Find_by_Program/Wells/default.htm and are also available from the USGS NWISWeb

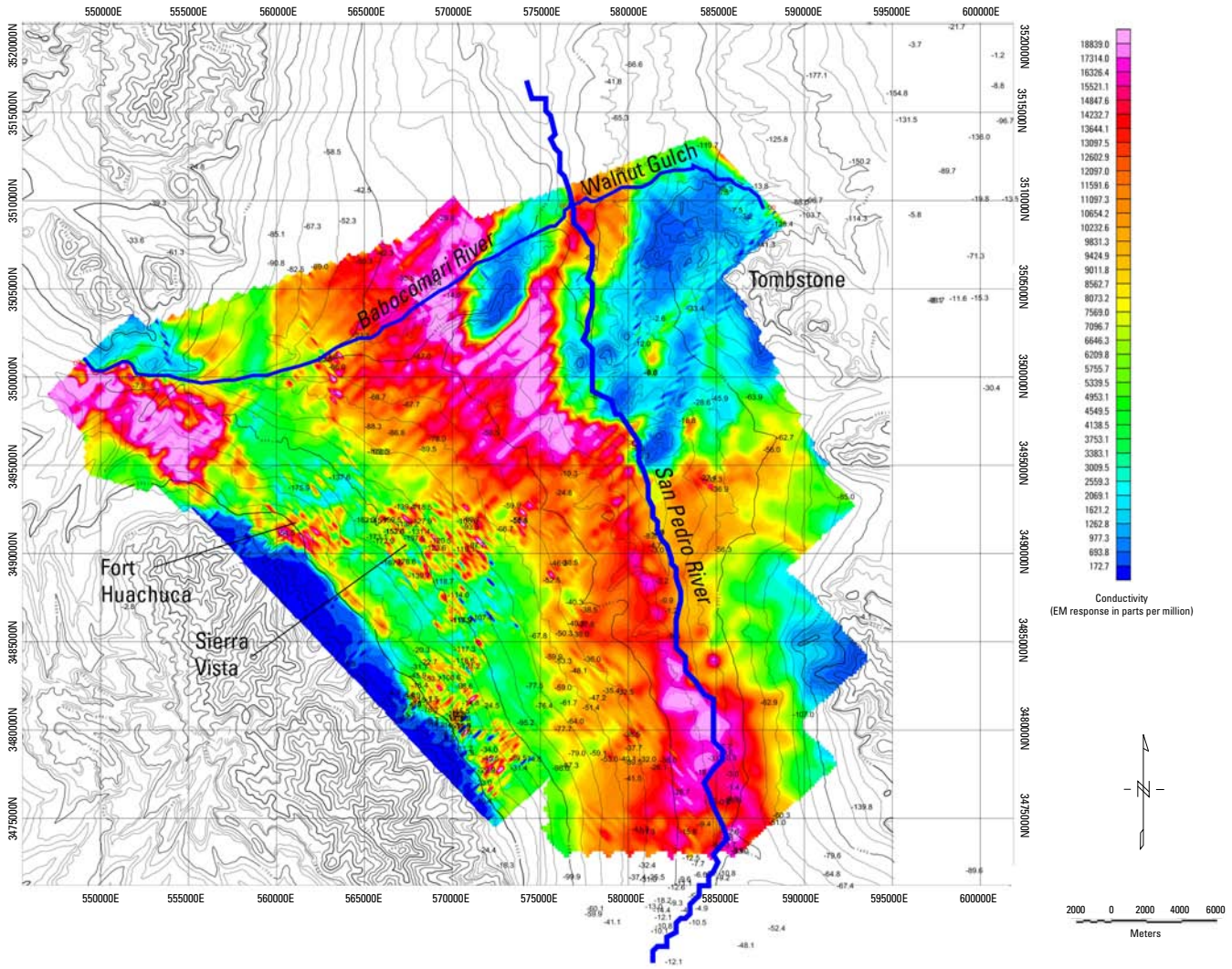

Base derived from U.S. Geological Survey Digital Elevation Model; contours show elevation in meters.

Figure 17. Depth to water table (black numbers) superimposed on shallow (1999 EM channel 10) conductivity data (colors) plotted on a map of the Fort Huachuca area, Arizona. The redder or warmer colors (zones of high conductivity) are inferred to represent water. The water-table data are from Maurice Tatlow (Arizona State Department of Water Resources, written commun., 1998; an edited version of Tatlow's data table can be found in appendix 1 of Bultman, Gettings, and Wynn, 1999). Depth to water table provided in feet, per Tatlow's data table (multiply feet by 0.3048 to obtain meters). Conductivity data from figure 14 are combined results from 1997 and 1999. An enlarged version of figure 17 is presented as plate 1 of this report.

(http://nwis.waterdata.usgs.gov/nwis). In general, there is good agreement between the water-table data and the conductivity data. The deeper water table that is 15 to 50 meters just east of Fort Huachuca and the Huachuca Mountains coincides with the green (weak electrical conductor) zones near Fort Huachuca. This area has already been identified as a deep unsaturated zone where the conductive water lies much deeper than it does farther east in the central part of the valley. Where the shallow electrical conductor (the red areas in the figure) strongly manifests, the water-table depths are in the 6- to 15-meter range. In the northeast, where the Tombstone Hills outcrop (the dark-blue zone in the upper right of the figure), there are very shallow water-table depths, but this is a zone where almost no water is present. Shallow (EM channel 10) aquifer extensions are also apparent on the east side of the San Pedro River, where they correlate closely with drainages that channel runoff westward from the Mule Mountains to the main regional aquifer.

The deep conductor (the hot-pink, low-resistivity zone seen in the EM channel 18 data of fig. 16) is apparently a deep, silt-and-clay-rich, high-porosity basin-center deposit. This clay-rich zone is also seen in the shallower channels (figs. 14 and 15). This is a water-saturated unit that accumulated in the San Pedro basin during late Miocene to Pliocene time (about 10 million to 2 million years ago). Weathered-out clays tend to concentrate more distally from their source rocks

than do sands and gravels, and so they tend to predominate in basin centers. The colors (bright purple in the CDTs discussed below) suggest that the deep conductor is less electrically conductive than the shallow aquifer above it. Apparently, this phenomenon is a subtle artifact of the airborne CDT inversion below about 150 to 200 meters. It is likely that the higher clay content in the central parts of the San Pedro basin (but west of the San Pedro River) has lower hydraulic conductivity. This clay content may cause at least some water flow in the upper San Pedro basin aquifer in a more northerly direction before discharging into the San Pedro River (for instance, via the Babocomari River).

In summary, the airborne EM survey appears to map where the water lies in the Sierra Vista subwatershed down to depths of 300 to 400 meters. Because overlying-sediment lithostatic pressure tends to reduce porosity with depth, most of the water lies in this depth range. Figures 14–16 by themselves cannot explain how the water from the Huachuca Mountains reaches the main regional aquifer, but CDT profiles suggest a deeper hydraulic connection beneath the mountain-front-following thick unsaturated zone. To draw reliable conclusions about ground-water flow, hydraulic data from wells in the area are required.

Conductivity Depth Transforms

Conductivity depth transforms (CDTs) are a proprietary product provided at extra cost by the airborne survey contractor. CDTs are calculated conductivity vs. depth sections derived by a mathematical transform (technically not an inversion process) of the 60-channel airborne electromagnetic in-phase/quadrature data acquired by the GEOTEM geophysical survey system, using an infinite half-space assumption. In earlier reports (Wynn and Gettings, 1997; Bultman, Gettings, and Wynn, 1999), CDT profiles were compared first with vertical electrical soundings (VES) carried out in the upper San Pedro basin and reported in Pool and Coes (1999), with available water-table data, and with short and long normal electrical logs from test wells on the Fort Huachuca military reservation. In general, we found good agreement between the CDT information and the VES and particularly good agreement with electrical well logs for the first 150 meters below the Earth's surface. We also found good agreement between the CDTs and other sources of San Pedro basin water information (for instance, Corell and others, 1996).

Figure 18 shows an example of a CDT, with an interpretation by Don Pool (USGS, Tucson, Ariz., written commun., 1999) superimposed; this figure was taken from 1997 survey line 122 and was chosen because 122 crossed close to test well 5, as discussed in Pool and Coes (1999). This geoelectrical section covers nearly 30 kilometers horizontally from southwest to northeast and up to 400 meters vertically (see pl. 2 for location of line 122 between L97114 and L97126). Blue indicates low conductivity, and warm colors represent high conductivity. In this area, the warm colors appear to map the water of the upper basin fill and lower basin fill (described in Brown and others, 1966, and Pool and Coes, 1999), as well as some of the Pantano Formation. The figure is topographically correct in that the elevations at Fort Huachuca (the southwest) are higher than the elevations at the San Pedro River (the northeast).

The shallow blue zone beneath and just east of Fort Huachuca is the thick unsaturated zone discussed on p. 21 and described in Pool and Coes (1999). Note the red beneath the zone in this CDT section; that is apparently water, probably saturated Pantano Formation sediments. Also note the continuity between the airborne EM conductor near the Huachuca Mountains on the left (red area labeled Pantano Fmn?) and the electrical conductor interpreted to be the regional aquifer (labeled UBF) in the center. This continuity or link was not apparent in the depth slices in figures 14–16. The CDTs, however, incorporated data from the longest time gates (deepest penetration) of the airborne EM data. The airborne EM system mapped a conductive (water-saturated) unit beneath the thick

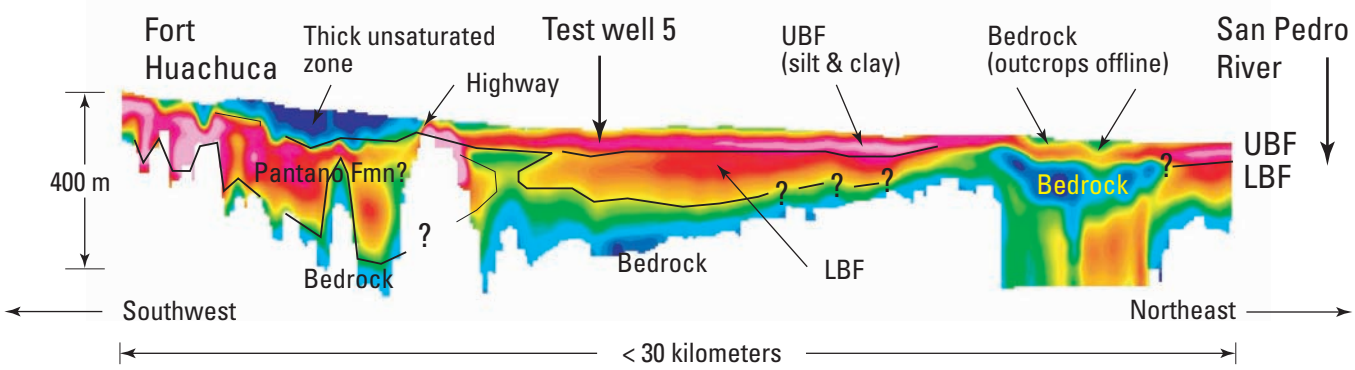

Figure 18. An example CDT profile from survey line 122, with an interpretation by Don Pool (USGS, Tucson, Ariz., written commun., 1999) superimposed. This figure is technically not an inversion of the airborne EM data, but a proprietary analytical calculation done by the contractor to convert the 60 channels of EM data into conductivity vs. depth over the length of survey line 122. LBF, lower basin fill; UBF, upper basin fill. Warm colors represent high conductivity.

unsaturated zone, showing apparent hydraulic connectivity at depth along the profile.

Just to the right of the blue, thick unsaturated zone, there is a thin red-purple area with white below it. This area is a high electrical conductivity zone that comes very close to the surface, perhaps reflecting the presence of effluent-recharge ponds found here. The U.S. Army National Environmental Protection Act Coordinator (Gretchen Kent, Fort Huachuca U.S. Army Garrison, oral commun., 1999) has indicated that there is significant water loss (up to 50 percent) in these ponds that cannot be explained by evapotranspiration. A possible interpretation is that some of this water is recharging the regional aquifer. A major highway crosses here, however, and so the possibility of cultural influence in the data at this point cannot be discounted. The white area underneath is caused by the presence of human electrical interference (pipelines and powerlines). The CDT algorithm cannot reliably calculate the deeper resistivities because the electrical noise from this cultural interference overwhelms the data below about 50–100 meters, and the plot software therefore leaves the area below the noise blank.

Farther northeast (to the center and right of fig. 18), there is a long, shallowing-to-the-right electrical conductor (deep red and purple) and a second deeper, red and orange zone. The shallow zone is likely water in the fine-grained upper-basin-fill part of the aquifer. The lower purple zone is the lower basin fill that is still part of the aquifer. The upper basin fill and lower basin fill are not separate but are parts of the same aquifer. Farther to the northeast, we see a shallow blue zone (labeled "Bedrock") with a very thin, barely subsurface red conductivity zone above it. These zones are the Tombstone Hills volcanic rocks, with a veneer of probably damp silt-clay making up a thin overlying layer of basin fill.

Figure 19 (from Bultman, Gettings, and Wynn, 1999) compares a conductivity depth transform with a resistivity log for test well 5 (see also Pool and Coes, 1999). Note that the horizontal axes in figures 19 and 20 are in units of resistivity. Most ground geophysical measurements are reported in resistivity units, whereas the strength of EM conductors is usually reported as conductivities. Resistivity and conductivity are related; resistivity is simply the inverse of conductivity (that is, resistivity = 1/conductivity). The short and long normal lateral electrical log in figure 19 shows resistivities that closely parallel the CDT results, but the CDT shows consistently higher resistivity (that is, the CDT curve lies to the right of the electrical log of the well). Below elevation 1,100 meters, the CDT resistivity values continue to increase and begin to diverge from the well-log resistivities. Apparently, the CDT gives approximately quantitative resistivity values (different by a small multiplicative factor) to about 150 meters depth and qualitative values (a slow, roughly linear increase) below this. It would seem that we should be able to "tune" the CDT algorithm to more perfectly match the actual electrical log resistivities over the entire survey area. This issue is discussed in further detail below.

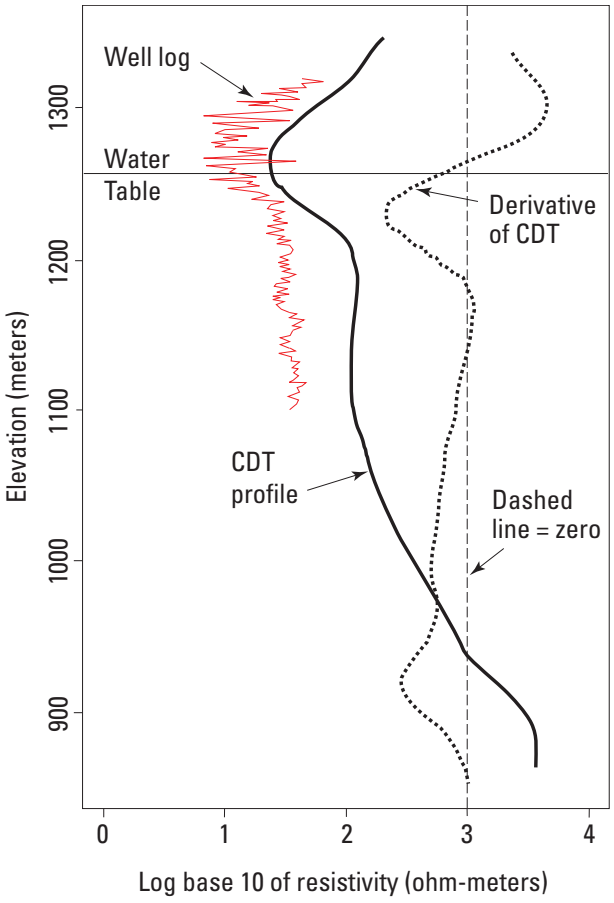

Figure 19. Graph showing comparison of resistivities derived from the airborne EM survey CDT with resistivities derived from a well log for test well 5. Also shown are the water table and a derivative of the CDT resistivity. The derivative of the digital CDT profile was plotted to indicate changes in slope of the profile. Where the derivative is zero, or when it displays slight negative slope, it is still possible to have increasing conductivity in the deeper portions of the profile. The CDT consistently demonstrates a higher resistivity at a given elevation than the well log, but, in general, the CDT resistivity profile seems well correlated with actual resistivity to depths of 150 meters (for example, elevations above 1,100 meters on the left-side scale). At depths greater than this, the well log and CDT resistivities begin to diverge. At this point, conductivities seem to be conservatively estimated or underestimated. From Bultman, Gettings, and Wynn, 1999.

Note that the first resistivity low of the CDT appears to mark the water table in figure 19. In fact, while this is generally the case over most of the San Pedro basin, there are some areas where the CDTs don't exactly mark the water table (for instance in a narrow zone near the mouth of Huachuca Canyon). Figure 20 (modified from Bultman, Gettings, and Wynn, 1999) shows a series of nine CDTs converted to resistivity-vs.-depth curves, correlated to the reported water table in nearby test wells. Six of the CDTs mark the water table closely, two mark the water table somewhat lower than where it was

measured, and one (the worst example we encountered in the Huachuca Canyon outflow area) seems to show the water table a full 100 meters below where it was measured. There is, however, some question about the accuracy of this water-table value (see p. 24). Some of the water-table values were older measurements taken when the water table was higher, so we can ascribe these few apparent discrepancies to either horizontal location imprecision between the CDT vertical section and the nearby well it is compared to or to older water-table measurements where the water is now further drawn down. The water-table values used for this report were always the most recent ones available.

There is also some suggestion (Mark Bultman, USGS, Tucson, Ariz.) written commun., January 2001) that the CDT algorithm may calculate the presence of the conductor above where it actually lies in cases of highly resistive (dry) overburden, again raising the question of whether we can tune the CDT algorithm better. While efforts are ongoing to resolve these occasional discrepancies, it is important to note that such discrepancies account for less than 5 percent of the surveyed area.

Figure 21 has been included to show another quality-control check of the data, in this case, the CDT inversion process. In this figure, a 1997 profile (1997 line 101) is compared with a nearly coincident 1999 profile (1999 line 214). The agreement is remarkable, considering that the position of the aircraft in three-dimensional space could never be made to coincide exactly.

Figure 22 (an enlarged version of this figure is presented as pl. 2 of this report) was generated to help readers visualize where the main electrical conductor (which the author believes generally correlates with the presence of water) lies in three dimensions; this is a CDT fence diagram. For selected airborne survey lines, entire CDTs have been scaled and laid down along the profile line. These CDTs are topographically corrected (that is, the white zone above a CDT on this fence diagram compensates for the fact that one end of the line may lie at a higher elevation). In these cases, the colored zones must be moved up to the surface in the viewer's mind. Doing this corrects a few apparent discrepancies; for instance, where the Babocomari River should coincide with a low-resistivity zone on the CDT that crosses or parallels it. This fence diagram thus can be considered a broad-brush three-dimensional map of the water underlying the San Pedro Valley in the survey area, with the caveats given above.

The CDTs in figure 22 show some interesting structural information. One example is a north-dipping conductor beginning at the Babocomari River on line L203 and extending down and north from the river. This conductor is almost certainly a water-filled, north-dipping fault system that controls the Babocomari. Another example can be seen in the middle of line L97–138. The Sawmill Canyon fault that is dashed through the basin fill on Drewes' map (1980) can be seen as a left-lateral offset in the conductor (fig. 14) and as an angled offset in the conductor in the middle of line L97–138 (fig. 22).

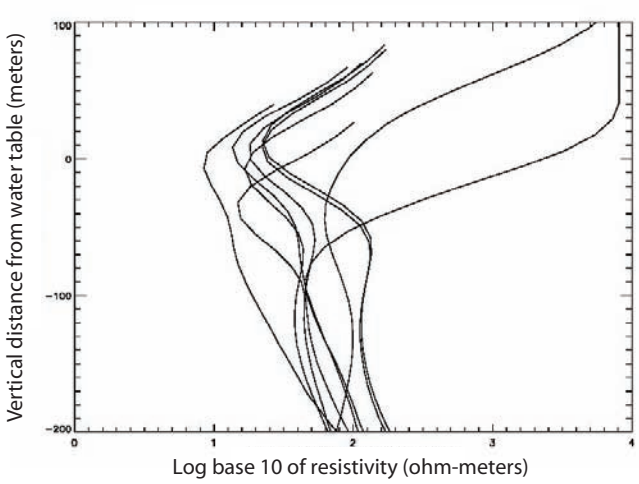

Figure 20. Graph showing CDT vertical profiles plotted against water-table information and well-resistivity data (log base 10 of resistivity) for nine test wells. All test wells were within 200 meters of a CDT location. Modified from Bultman, Gettings, and Wynn, 1999.

In Bultman, Gettings, and Wynn (1999), some interesting relations among the digital CDTs, the well resistivity logs, and the water tables were observed. These observations (listed below) appear to be applicable to the entire 1997/1999 dataset.

1. The digital CDTs consistently demonstrate a slightly higher resistivity at a given depth than the short and long normal well logs. Some of this difference may be due to an elevation problem that was discovered and reported in the 1997 digital CDTs, and some of it may be due to parameters selected by the contractor in the CDT algorithm. The elevation problem has been corrected in the 1997 data and did not appear in the 1999 data.
2. The shape of the CDTs matches the general shape of the well logs in most cases for the first 150 meters depth.
3. For most of the test wells, the CDT-derived upper conductivity maximum/resistivity minimum seems to correlate well (within the vertical resolution of the CDTs) with the water table. In a few places, notably near the mouth of Huachuca Canyon, the conductivity maximum suggests that the water table is lower than the water table in nearby wells. This finding may be due to the significant horizontal displacement between the wells and the CDT soundings or to outdated water-table information or even to a calibration issue with the CDT algorithm in zones of highly resistive overburden. The author believes that the cause is likely a combination of all three.

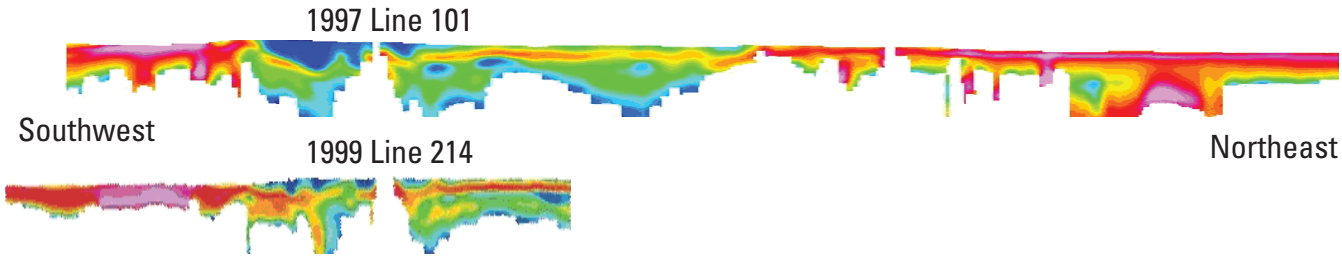

Figure 21. Comparison of two CDT profiles (1997 line 101 and 1999 line 214) that approximately coincide. The profiles agree well despite the fact that the position of the aircraft in the two overflights could never be made to coincide exactly. Line 214 is also plotted in plate 2 and figure 22.

4. The CDT resistivity profiles, when converted to conductivity vs. depth, correlated well with actual well-log resistivity to depths of about 150 meters. At depths below 150 meters, resistivities reported in the CDTs increase with greater depth over the resistivities measured by well logging. This finding led the author to consider the possibility of "tuning" the CDT algorithm to match the well logs down to 400 meters depth, as discussed in detail below.

Conductivity vs. Depth Conversion Systems—The Inversion "Tuning" Issue

One product of the AEM survey is a conductivity vs. depth section derived by a mathematical calculation of the 60-channel airborne electromagnetic data acquired by the geophysical survey system. The airborne geophysical contractor, Geoterrex-Dighem, refers to these calculations as conductivity depth transforms or CDTs. Wolfgram and Karlik (1995) described the mathematical technique used to obtain the CDTs; however, Geoterrex-Dighem considers the actual algorithm proprietary. While not technically a true inversion, the technique produces results similar to an inversion based on the diffusion equation, yet requires much less computation time because it is a forward, or analytical, calculation.

Earlier, we observed the generally good correlation between well logs and the CDT resistivity values (see p. 24); this correlation helps to establish the veracity of the CDT algorithm. The apparent close correlation between CDT resistivities and electrical logs in wells down to depths of 150 meters is encouraging; however, the increasing disparity or difference below 150 meters is problematic. To test the accuracy of the CDT algorithm, the USGS purchased an EM inversion software package called "EM Flow" from ENCOM. ENCOM is an Australian Government/private-industry geophysical consortium; the inversion method used in the software is documented in Macnae and others (1991). Approximately 1 person-month was spent reformatting the 1999 airborne EM data and revising the software so that it could invert data from parts of the 1999 airborne geophysical survey.

The survey line chosen for the test comparison was a separate 10-kilometer-long profile flown parallel to the Mexican border and south of the combined Geoterrex-Dighem 1997/1999 surveys coverage. This comparison survey line is called the "Mexico Border Line" here and in figure 2 (see L1000 Mex on pl. 2 and fig. 22). The Mexico Border Line is important because a large part of the San Pedro basin drainage lies south of the Mexican border. This line provides continuity between the aquifer surveyed for this report and that part of the San Pedro aquifer lying south of the border. It is reasonable to assume that ground water flows across the border, down-drainage toward the north. The extent to which an estimated volume of formerly Mexican ground water contributes to stream flow on the American side of the San Pedro River, however, cannot be quantified at this time. The perennial flow in the San Pedro River north of the border is influenced by the geometry of the channel alluvium and the volume of bank storage present.

Operations at Cananea, the large porphyry copper mine that lies in the upper San Pedro drainage in Mexico withdraw a considerable amount of water from the upper San Pedro drainage. The mining company Grupo Mexico has acknowledged the ongoing withdrawal from the upper San Pedro aquifer of more than 15 million cubic meters of water per year for the Cananea mine and its local operations (José María Guerra-Limón, Reserva Forestal Nacional y Refugio de Fauna Silvestre "Ajos-Bavispe," Hermosillo, Mexico, oral commun., 2000). The withdrawal apparently began in the 1940s and accelerated during the 1950s and 1960s to its present level. It is reasonable to assume that this withdrawal could have a significant effect on the ground-water system on the American side of the border. Note that the Cananea mine is one of many entities withdrawing water from the upper San Pedro aquifer in Mexico, including large communal farms (ejidos) and towns.

Figure 23 compares the Geoterrex-Dighem CDT (conductivity-depth-transform) profile and the ENCOM CDI (conductivity-depth-inversion) profile for the Mexico Border Line. Figure 23*A* shows the original EM Flow inversion (CDI) of the normal off-time gates that the EM Flow software was configured to deal with. These time gates are well suited to

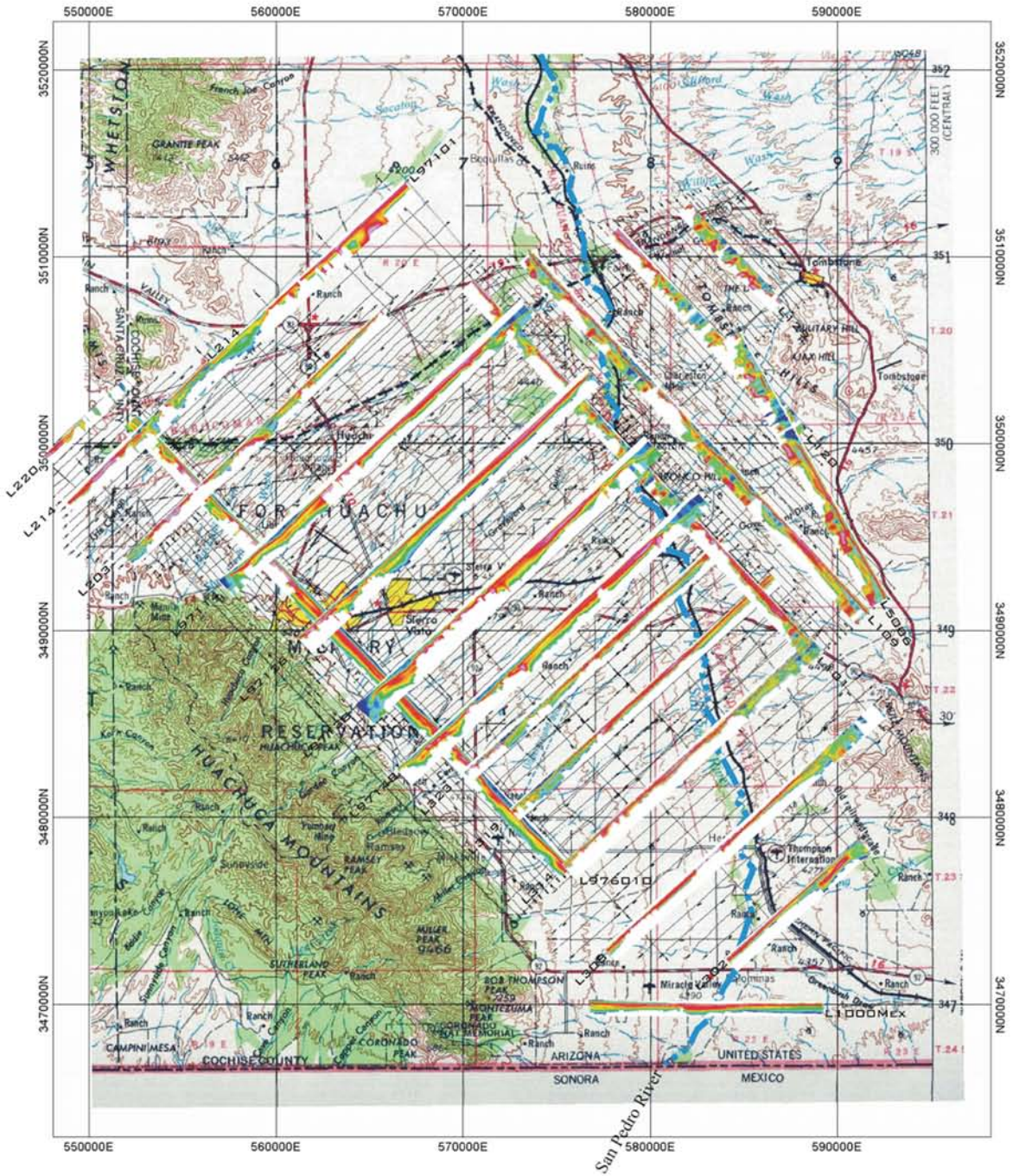

Figure 22. Conductivity vs. depth fence diagram (where approximately every 10th CDT is laid down along its survey line) superimposed on a topographic map of the Fort Huachuca area, Arizona. This diagram permits the reader to view a three-dimensional representation of the conductivities as a function of depth on a two-dimensional sheet. The data portrayed are from the 1997 and 1999 airborne EM surveys (Geoterrex-Dighem, 1997, 1999). An enlarged version of figure 22 is presented as plate 2 of this report.

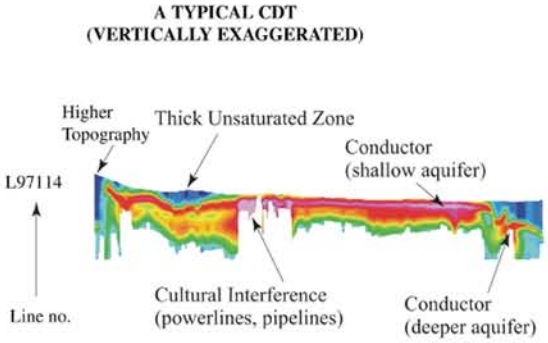

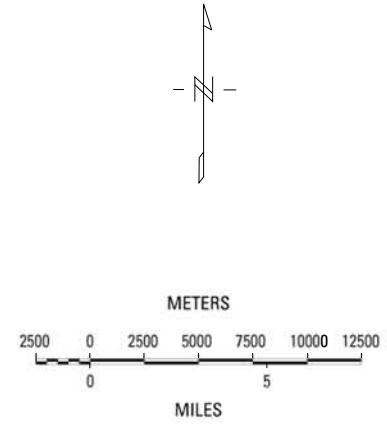

Base from 1:250,000-scale U.S. Army Topographic Command (KCSX); revised by U.S. Geological Survey, 1969; contours show elevation in feet. Data superimposed from San Pedro (1997) and Tombstone (1999) airborne geophysical surveys (Geoterrex-Dighem, 1997, 1999).

defining details in the upper section of the profile but do not sample far out into the late-time windows acquired by Geoterrex-Dighem's GEOTEM system. Figure 23*B* shows the original channel-by-channel EM data, for reference. Figure 23*C* is the EM Flow result when the sampling time gates are extended back into the on-time of the transmitter (for a closer reference to the transmitted signal strength) and as far down the off-time window as the software could handle. This method sampled as deeply beneath the ground surface as possible for a better comparison to the Geoterrex-Dighem CDT profile. Figure 23*D* shows the Geoterrex-Dighem CDT profile.

Comparisons between the Geoterrex-Dighem CDTs and the EM Flow CDIs show the following:

1. The EM Flow inversion for a single profile takes up to 10 minutes to complete on a fast Pentium-III computer. The CDI process generally requires several runs, then color scaling to reduce color saturation to bring out details. The CDT analytical calculation (that is, a forward calculation), on the other hand, requires only a few seconds. The heavy calculation burden and other inherent limitations make the 1999 EM Flow software an interesting research tool but poorly suited to production processing of large airborne EM surveys.

2. The EM Flow inversion provides fine resistivity detail in the upper 50–70 meters below the Earth's surface—substantially more detail than the Geoterrex-Dighem CDT provides.

3. The EM Flow inversion, when extended to include early and late time gates (fig. 23*C*), agrees well with the CDT analytical conversion of the EM data (fig. 23*D*). The minor disparities are caused by the relative strengths of the two conversion methods.

4. The EM Flow results do not reach as deep as the Geoterrex-Dighem analytical CDT solution. In figure 23*D,* we see a second, deeper conductive unit (possibly another deeper water body) on the left (west) side of the profile. We can see only a hint of this deeper, second water body in the EM Flow inversion. This water body is not clearly seen on the EM Flow CDI because the software could not use the longest time gates in the data.

5. Silts and clays generally tend to collect distally from the source rocks from which they weathered. Along the Mexico Border Line, applying this fact suggests that clays would tend to collect in the center of the area shown in figure 23, near the San Pedro River (between reference UTM coordinates 580000E and 586000E). Sands and gravels, on the other hand, would likely predominate on the edges of a basin. One could then infer that both the shallow and deeper electrical conductors seen on the left side of figure 23*D* probably represent accessible bodies of water. An observer using the CDT would thus understand that any water well located in this area should be extended below the first (shallow) electrical conductor, through the apparent aquiclude separating it from the underlying electrical conductor, and into the apparent second, deeper water body. This guidance would not be available if the interpreter used only the EM Flow CDI inversion results.

6. Around location 582000E (the east component of the UTM coordinates) on the Mexico Border Line, there is an apparent offset in the high-conductivity layers (warm colors in fig. 23*C,D*). This offset is a previously unknown feature and probably represents a normal fault that influenced the accumulation of alluvial materials. As such, the apparent offset may simply reflect an increase in the thickness of the basin fill on the east side.

Summary of Interpretations

Interpretations Related to the Hydrology of the Upper San Pedro Drainage Derived from the Airborne EM and Magnetic Data

When combined with the hydrologic analysis of Pool and Coes (1999), the 1997 and 1999 airborne geophysical surveys provide sufficient information to draw the following conclusions:

1. The EM conductivity maps (figs. 14–16) and the CDT profiles (figs. 18, 21–23, pl. 2) show subsurface conductivities in an area of about 1,000 square kilometers. This kind of subsurface imaging is possible because the local ground water is quite conductive (Pool and Coes, 1999, pl. 3). While clays are also known to contribute to an increased conductivity, they cannot be the dominant factor in the conductivity images we see in these figures for reasons explained above (see p. 18–19). Nevertheless, for conductivities above 300–500 μS/cm, clays definitely have contributed to the values measured. Consequently, the airborne-EM-derived conductivity maps provide a high-resolution, as well as a broad-brush, image of the presence of ground water in the Sierra Vista subwatershed of the upper San Pedro regional aquifer, especially when combined with existing lithologic and hydrologic information. The parameters for the airborne EM surveys were optimized for maximum penetration in the San Pedro Valley (that is, about 400 meters). In the absence of human cultural interference, the CDT profiles generally map most of the underlying water (note the closure, or bottoms, of the electrical conductors in the CDTs).

2. The airborne EM data provide a static image of the subsurface electrical conductor inferred to be the regional aquifer. Figures 14–16 effectively provide three depth

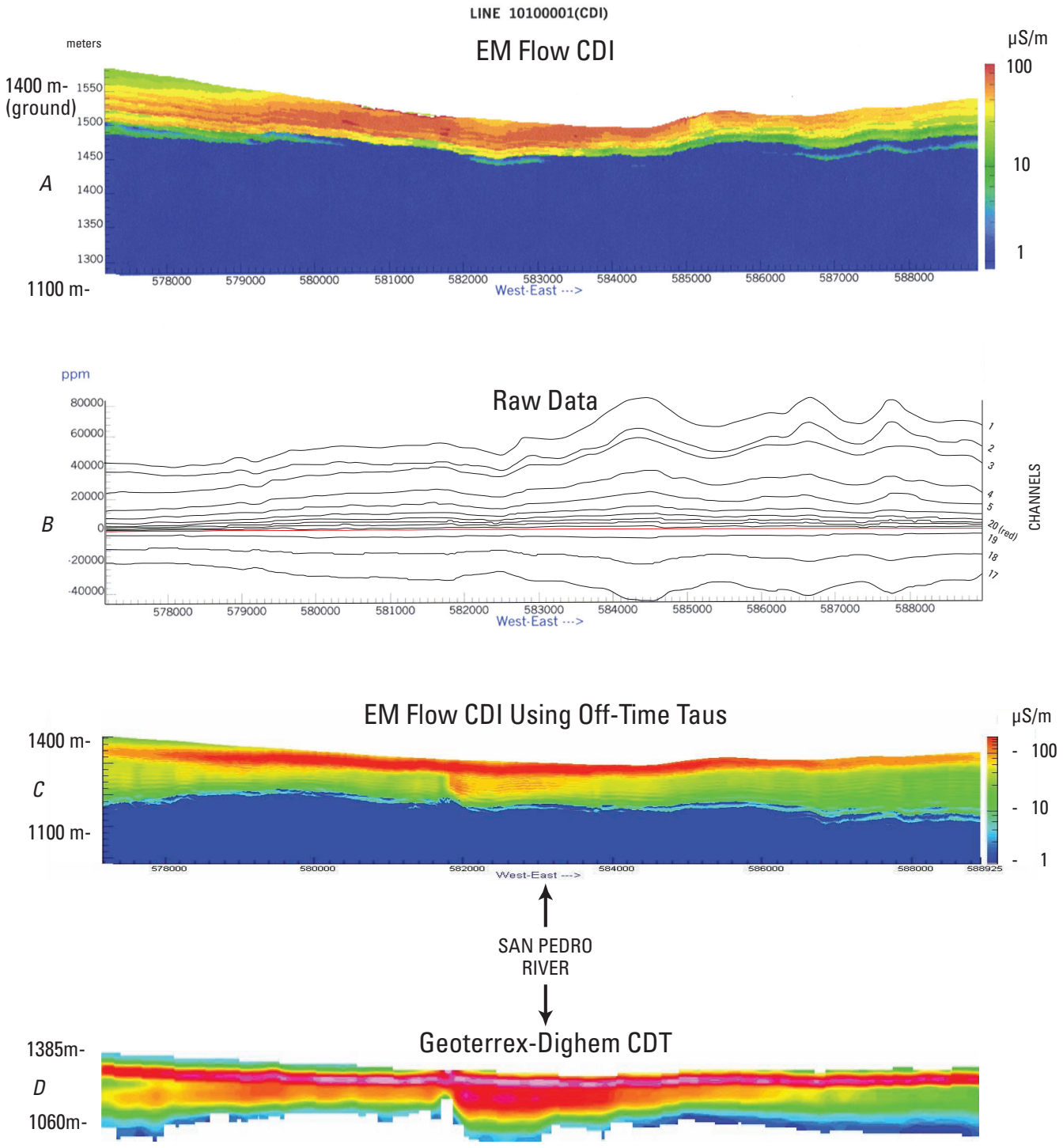

Figure 23. A comparison of a true inversion of the 60-channel EM data (using an EM Flow CDI) with a Geoterrex-Dighem CDT profile for the same survey line, the so-called Mexico Border Line, acquired approximately 3 kilometers north of the Mexican border (see line L1000 Mex in fig. 22). *A*, A normal (on-time taus only) inversion. *B*, Original channel-by-channel EM raw data presented for comparison. *C*, The EM Flow inversions using off-time taus (providing a closer reference to the transmitted signal and thereby allowing deeper penetration). *D*, Analytical CDT profile. Warm colors represent high conductivity. Units: m, meter; µS/m, microsiemens per meter; ppm, parts per million.

slices of this electrical conductor beneath the study area. The airborne EM images and CDTs do not directly provide information about ground-water flow, although an experienced hydrologist can draw some educated inferences from the images.

3. In many places, the CDTs provide structural information about the subsurface, such as the north-dipping, water-saturated fault system controlling the Babocomari River (the northward-dipping electrical conductor beginning at the Babocomari River on line L203 in fig. 22 and pl. 2).

4. The airborne EM conductivity images suggest substantially reduced porosity beneath the Tombstone Hills volcanic field, over which the San Pedro River flows for about 30 percent of its length in the northern part of the survey area. In this zone, at least, hydraulic communication is substantially reduced between the San Pedro River and the regional aquifer.

5. The upper-basin-fill sediments in the center of the San Pedro Valley appear to be water saturated. The apparent offset of the main conductor to the west of the river, combined with basic sedimentary principles that place the silts and clays more in the center of a basin, suggest the presence of a large silt-clay body just to the west of the river. Both the CDTs and well-log data support this theory. This electrically conductive unit, which roughly parallels the river but lies to its west, has sands and gravels both overlying and underlying it and significantly influences the ground-water flow in the regional system (Pool and Coes, 1999).

6. Almost 4 million cubic meters of ground water is estimated to flow from Mexico into the Arizona part of the basin each year (Freethey, 1982). The Cananea mine complex in Mexico, which withdraws more than 15 million cubic meters of water each year, must have a significant effect on water flowing in the San Pedro River in Arizona. A further increase in withdrawal in Mexico will almost certainly affect the San Pedro National Riparian Conservation Area.

7. The magnetic depth-to-source maps generated as part of this study reveal that there are several deep sections of the upper San Pedro basin in the study area (for example, beneath Huachuca City and beneath the Palominas area near the Mexican border; figs. 11 and 12). These deep zones are filled with sediment and, in places, saturated with water. Because of overlying lithostatic pressure, which generally reduces the porosity, the bulk of the regional aquifer probably lies within the 400-meter-depth range of the airborne EM system. Nevertheless, the large volume of sediment that these huge "potholes" represent in the crystalline rock basement must contribute substantially to the bank storage volume in the Sierra Vista subwatershed.

8. The magnetic depth-to-source map (fig. 11) also shows that most of the San Pedro River in the southern 70 percent of the study area (south of the Tombstone Hills) has only 100 to 200 meters of sediment underlying it. This relatively thin, silt-and-clay-rich section of alluvium implies lower transmissivity in the immediate vicinity of the river in this segment south of 3493000N. Lines L323, L319, and L314 of figure 22 and plate 2 support this finding by showing only a thin electrical conductor (that is, a thin, shallow water body) on the east side of each profile. According to Don Pool, "This feature likely also influences the movement of ground water in the system" (USGS, Tucson, Ariz., written commun., January 2001).

Observations about the Geology of the Upper San Pedro Drainage Derived from the EM and Magnetic Data

General geologic observations from the combined 1997 and 1999 airborne geophysical surveys include the following:

1. The upper San Pedro basin is bounded on the southwest by the Nicksville fault (Drewes, 1980), a high-angle basin-margin fault marking the eastern edge of the Huachuca Mountains that is apparent in the magnetic data. The airborne EM data (figs. 14–16) show the Sawmill Canyon fault (Drewes, 1980, 1996) as a subtle left-lateral offset in the shallow conductor in the middle of the basin. The Babocomari River appears to coincide with a north-dipping fault evidenced as a narrow dipping conductor in the CDT data for line L203.

2. A bedrock high in the Sierra Vista area extends eastward about 10 kilometers from the Huachuca Mountains into the basin. Figure 11 shows this feature in the inverted magnetic data and in the CDT data as a rise in the near-surface low-resistivity zone. The presence of this high has been verified by well D(21-20)35abb, located near Fry Boulevard in Sierra Vista (Gettings and Houser, 2000).

3. South of the Sierra Vista bedrock high, the basin is complex but includes a large Basin-and-Range-following basement low that appears to extend south into Mexico from the Palominas area. The gravity-based model agrees closely with the magnetic model but, with fewer data points, has a much lower resolution (see also Halvorson, 1984).

4. To the east of the basin-bounding fault near the Huachuca Mountains and east of the Sierra Vista bedrock high, the basin remains deep until it approaches the Tombstone Hills. The relation between the basin sediments and the bedrock in the Tombstone Hills area is complex and may be both stratigraphic (intercalated volcanic flows in the sedimentary stack) and fault bounded. This region correlates to the mapped Tombstone caldera margin (Moore, 1993).

Observations about the Geophysical Methods, Including the CDT Conversion Process

The following are observations about the CDT algorithm and the conversions released by Geoterrex-Dighem (1997, 1999):

1. The Geoterrex-Dighem CDT conductivities appear to map the presence of water to about 150 meters depth over most of the survey area. Below about 150 meters depth, the CDT conductivities diverge with increasing depth (toward lower conductivities) from values measured in well logs. In this zone, the CDTs still appear to provide at least qualitative data on the presence or absence of water. In a few areas, the water-table depths diverge from what the CDTs seem to show, notably in a narrow zone near the mouth of Huachuca Canyon. This phenomenon may be due to (a) out-of-date water-table information in a sharply fluctuating recharge channel, (b) horizontal registration errors between wells and the CDT profile, or (c) a subtle calibration issue with the CDT algorithm apparent only in areas of highly resistive overburden. The available evidence suggests a combination of all three.
2. The bedrock under the basin sediments is generally visible in the EM data only where it outcrops or is overlain by less than about 300–400 meters of alluvium. The crystalline bedrock, however, is easily mapped by the airborne magnetic data converted through the Euler deconvolution algorithm. In a few cases, magnetic volcanic flows and volcanosedimentary units deposited in the middle of the sediment stack above the crystalline basement make the basement appear to be locally shallower; for instance, the apparent ridge in the middle of the Huachuca City basement low (which according to the gravity data is a single, deep subbasin in the San Pedro Valley).
3. The CDI inversion process (that is, the EM Flow solutions) appears to verify the CDT analytical conversion process. Well-log information generally supports the veracity of the CDTs and the conductivity maps shown in figures 14–16.

Acknowledgments

Gretchen Kent, the National Environmental Protection Act Coordinator for the U.S. Army Garrison at Fort Huachuca, Ariz., arranged for funding for the airborne geophysical surveys and for the analysis, helped coordinate the surveys with the base commanders, provided strong encouragement throughout this effort, and provided a review. These surveys were designed and carried out under U.S. Geological Survey (USGS) supervision at the request of the Environmental and Natural Resources Division at the Fort Huachuca U.S. Army Garrison, which funded them. Fort Huachuca also provided previous data and reports, funding to assist with the analysis and interpretation of these data, and logistical support to the flight crews. Fort Huachuca's goal in assisting with these studies was to provide objective, state-of-the-subsurface knowledge to those agencies and organizations trying to plan and manage water resources in the region.

Mark Gettings and Floyd Gray of the USGS invited the author (Jeff Wynn) to become involved in the Southwest Resources project within the USGS and take on this particular subtask. During the 1997 and 1999 surveys, the author served on site as the contracting officer's representative, working with flight engineers and the data-reduction team to assure that quality-control procedures were strictly adhered to.

Mark Bultman (USGS) provided independent calculations to support this work. Jean Lemieux (Geoterrex-Dighem; the company is now part of Fugro World Wide) provided additional insight and directed the generation of the conductivity depth transforms (CDTs); he offered much helpful advice during the interpretation phase of this survey, particularly on issues related to gain and system sensitivity. Vic Labson (USGS) provided valuable insight in setting up both airborne surveys and, in particular, in setting the EM system sampling parameters.

This report benefited significantly from reviews by Don Pool, Bill Steinkampf, and Mark Bultman (all of the USGS, Tucson, Ariz.). In addition, Tom Reilly (USGS, Reston, Va.) and Mark Anderson (USGS, Tucson, Ariz.) also provided reviews.

References Cited

Andreasen, G.E., Mitchell, C.M., and Tyson, N.S., 1965, Aeromagnetic map of Tombstone and vicinity, Cochise and Santa Cruz Counties: Washington, D.C., U.S. Geological Survey Open-File Report, scale 1:125,000.

Blakeley, R.J., 1995, Potential theory in gravity and magnetic applications: New York, Cambridge University Press, 441 p.

Brown, S.G., Davidson, E.S., Kister, L.R., and Thomsen, B.W., 1966, Water resources of Fort Huachuca Military Reservation, southeastern Arizona: U.S. Geological Survey Water-Supply Paper 1819–D, 57 p.

Bultman, M.W., Gettings, M.E., and Wynn, Jeff, 1999, An interpretation of the 1997 airborne electromagnetic (AEM) survey, Fort Huachuca vicinity, Cochise County, Arizona, with digital data: U.S. Geological Survey Open-File Report 99–7–A, one CD-ROM, and U.S. Geological Survey Open-File Report 99–7–B (a simplified and shortened version of Open-File Report 99–7–A), available online at http://geopubs.wr.usgs.gov/open-file/of99-007-b/.

Corell, S.W., Corkhill, E.F., Lovvik, D., and Putman, F., 1996, A groundwater flow model of the Sierra Vista subwatershed of the upper San Pedro basin—Southeastern Arizona: Arizona Department of Water Resources Report No. 10, 107 p.

Defense Mapping Agency, 1994, Fort Huachuca Military Installation Map: Defense Mapping Agency Arizona map edition 3-DMA, Series V798S, Fort Huachuca MIM, scale 1:50,000.

Dohrenwend, J.C., Gray, Floyd, and Miller, R.J., 2001, Processed Landsat Thematic Mapper satellite imagery for selected areas within the U.S.–Mexico borderlands (false color composite image, Path 35 Row 38; acquired on 24 June 1997 (band 7–red; band 4–green; band 2–blue)): U.S. Geological Survey Open-File Report 00–309, version 1.0, three CD-ROMs. (Also available online at http://geopubs.wr.usgs.gov/gov/open-file/of00-309/.)

Drewes, Harald, 1980, Tectonic map of southeast Arizona: U.S. Geological Survey Miscellaneous Investigations Series Map I–1109, scale 1:125,000.

Drewes, Harald, 1996, Geologic maps of the Coronado National Forest, southeast Arizona and southwest New Mexico: U.S. Geological Survey Bulletin 2083–B, p. 17–41, pls. 2–4.

Driscoll, F.G., 1986, Groundwater and wells: St. Paul, Minn., Johnson Division, 1,089 p.

Environmental Engineering Consultants, 1996, EEC Project No. 1422.34, Report prepared for the Directorate of Engineering and Housing, Environmental Division, USAG Fort Huachuca, ATZS-EHB, Fort Huachuca, Arizona, 85613–6000: 29 p.

Flanigan, V.F., and Wynn, J.C., 1979, Preliminary report of geophysics ground follow-up of the 1977 airborne survey in the Wadi Bidah district, Kingdom of Saudi Arabia: Saudi Arabian Project Report, Directorate General of Mineral Resources, Ministry of Petroleum and Mineral Resources, Jeddah, Saudi Arabia, Interagency Report IR–348, 54 p.

Freethey, G.W., 1982, Hydrologic analysis of the upper San Pedro basin from the Mexico-United States international boundary to Fairbank, Arizona: U.S. Geological Survey Open-File Report 82–752, 64 p.

Geoterrex-Dighem, 1997, Logistics and processing report of the airborne magnetic and GEOTEM electromagnetic survey over the Fort Huachuca Military Reservation, Cochise County, Arizona: Ottawa, Canada, Geoterrex-Dighem, 14 p., 10 apps.

Geoterrex-Dighem, 1999, Logistics and processing report of the airborne magnetic and GEOTEM electromagnetic multicoil survey over the Fort Huachuca Military Reservation, Cochise County, Arizona: Ottawa, Canada, Geoterrex-Dighem, Job No. 521, 13 p., 10 apps.

Gettings, M.E., 1996, Aeromagnetic, radiometric, and gravity data for Coronado National Forest, *in* du Bray, E.A., ed., Mineral resource potential and geology of Coronado National Forest, southeastern Arizona and southwestern New Mexico: U.S. Geological Survey Bulletin 2083–D, p. 70–101.

Gettings, M.E., and Houser, B.B., 1995, Preliminary results of modeling the gravity anomaly field in the upper San Pedro basin, southeastern Arizona: U.S. Geological Survey Open-File Report 95–76, 9 p.

Gettings, M.E., and Houser, B.B., 2000, Depth to bedrock of the upper San Pedro Valley, Cochise County, southeastern Arizona: U.S. Geological Survey Open-File Report 00–138, 34 p.

Gettings, P.E., and Gettings, M.E., 1996, Modeling of a magnetic and gravity anomaly profile from the Dragoon Mountains to Sierra Vista, southeastern Arizona: U.S. Geological Survey Open-File Report 96–288, 15 p., 3 pls.

Halvorson, P.H.F., 1984, An exploration gravity survey in the San Pedro Valley, southeastern Arizona: Tucson, Ariz., University of Arizona, Master's thesis, 70 p.

Ingebritsen, S.E., and Sanford, W.E., 1998, Groundwater in geologic processes: New York, Cambridge University Press, 341 p.

Keller, G.V., and Frischknecht, F.C., 1966, Electrical methods in geophysical prospecting: Oxford, Pergamon Press, 517 p.

Macnae, J.C., Smith, Richard, Polzer, B.D., Lamontagne, Y., and Klinkert, P.S., 1991, Conductivity-depth imaging of airbourne electromagnetic step-response data: Geophysics, v. 56, no. 1, p. 102–114.

Moore, R.B., 1993, Geologic map of the Tombstone volcanic center, Cochise County, Arizona: U.S. Geological Survey Miscellaneous Investigations Series Map I–2420, scale 1:50,000.

Pool, D.R., and Coes, A.L., 1999, Hydrogeologic investigations of the Sierra Vista subbasin of the upper San Pedro River basin, Cochise County, Arizona: U.S. Geological Survey Water-Resources Investigations Report WRIR 99–4197, 47 p., 3 pls.

Reid, A.B., Allsop, J.M., Granser, H., Millett, A.J., and Somerton, I.W., 1990, Magnetic interpretation in three dimensions using Euler deconvolution: Geophysics, v. 55, p. 80–91.

U.S. Army Corps of Engineers, Sacramento District, 1972, Final Report—Test well drilling and study of hydrogeologic conditions, Fort Huachuca, Cochise County, Arizona: U.S. Army Corps of Engineers, Sacramento District, 21 p., 7 enclosures.

U.S. Army Corps of Engineers, Sacramento District, 1974, Supplemental report—Test well drilling and study of hydro-

geologic conditions, Fort Huachuca, Cochise County, Arizona: U.S. Army Corps of Engineers, Sacramento District, 19 p., 8 enclosures.

Wolfgram, P., and Karlik, G., 1995, Conductivity-depth transform of GEOTEM data: Exploration Geophysics, v. 26, p. 179–185.

Wynn, J.C., and Gettings, M.E., 1997, A preliminary interpretation of the 1997 airborne electromagnetic (EM) survey over Fort Huachuca, Arizona, and the upper San Pedro River basin: U.S. Geological Survey Open-File Report 97–457, 22 p.

Wynn, Jeff, 2002, Evaluating groundwater in arid lands using airborne magnetic and airborne electromagnetic methods—An example in the southwestern U.S. and northern Mexico: The Leading Edge, v. 20, no. 12, p. 62–65.

Wynn, Jeff, Pool, Don, Bultman, Mark, Gettings, Mark, and Lemieux, Jean, 2000, Airborne EM as a 3-D aquifer-mapping tool, *in* Symposium on the Application of Geophysics to Engineering and Environmental Problems, 13th, Arlington, Va., Proceedings: Denver, Colo., Environmental & Engineering Geophysical Society, p. 93–100.

ISBN 978141130012